RICE UNIVERSITY

Influence of Citrate Ligands on Ferric Hydroxide Nucleation at Low Molar Ratios: Application for Arsenic Removal

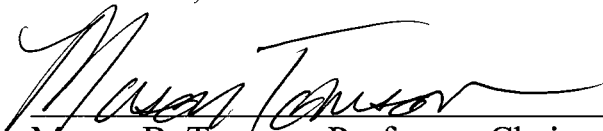By

Nan Zhang
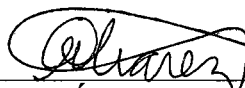
A THESIS SUBMITTED
IN PARTIAL FULFILLMENT OF THE
REQUIREMENTS FOR THE DEGREE

Master of Science

APPROVED, THESIS COMMITTEE:

Mason B. Tomson, Professor, Chair
Civil and Environmental Engineering

Pedro J. Álvarez, George R. Brown
Professor, Civil and Environmental
Engineering

Philip B. Bedient, Herman Brown Professor,
Civil and Environmental Engineering

HOUSTON, TEXAS
APRIL 2010

UMI Number: 1485987

ABSTRACT

Influence of Citrate Ligands on

Ferric Hydroxide Nucleation at Low Molar Ratios:

Application for Arsenic Removal

By

Nan Zhang

The U.S. EPA recommends adding of 5-25mg/L ferric salt to remove arsenate (V) at pH 5 to 8 in water treatment plants. Citrate has been proven to inhibit ferric hydroxide floc formation and corresponding arsenic adsorption. Although most research has been conducted at high molar ratios of citrate to iron, low molar ratios were used in this work and the inhibition of floc formation remained constant above a molar ratio of 0.05. Nucleation kinetics of ferric hydroxides and arsenic removal was investigated in the presence of citrate at low molar ratios (citrate/Fe ranging from 0 to 0.28). At concentrations found in natural waters (4.5-25μM), citrate effectively inhibited ferric hydroxide nucleation and precipitation by forming a non-crystalline macromolecular complex (FeO(Fe$_3$O$_{12}$H$_3$)Cit) detected in aqueous phase by electrospray ionization mass spectrometry (ESI-MS). Arsenate removal by nano magnetite was also retarded by a low concentration of citrate. The effectiveness of citrate was more significant at higher pH values. Possible mechanisms of citrate inhibition at low molar ratios were compared and discussed. This research demonstrated that the citrate impact upon arsenate removal should be considered when using the iron coagulation and precipitation method in water treatment plants.

ACKNOWLEDGEMENTS

TABLE OF CONTENTS

LIST OF FIGURES

LIST OF TABLES

1 Introduction

Arsenic is widely known to be a naturally occurring and highly toxic contaminant in drinking water within the Unites States and around the world. High risk of cancers, neurological disorders and skin damage have been linked to chronic intake of arsenic at both high and low concentrations. In America, arsenic is the second most important contaminant of concern (after lead), detected at 568 superfund sites. (Ahmed et al. 2001; U.S.EPA 2002) Drinking water, especially groundwater, is the primary medium that introduces arsenic into the biosphere, although arsenic can be mobilized through both natural and anthropogenic activity. (Yu et al. 2003; Feenstra et al. 2007; Pelley 2009) In response to increased awareness and concern regarding the effects of arsenic, the U.S. EPA set and enforced a maximum contaminant level (MCL) for arsenic of 10µg/L in January 2006.

Precipitation and coagulation by iron or aluminum salts is the most common large scale ex-situ arsenic removal technology, and it is a low-cost, point-of-use drinking water treatment used in developing cities like Bangladesh in India.(Hering et al. 1997; Fields et al. 2000; Ahmed et al. 2001; Betts 2001; U.S.EPA 2002) However, this routine chemical addition and sludge removal method has two disadvantages: contaminant sludge residuals disposal problem and the influence of competitive adsorption of other anion, such as phosphate, dissolved silicon, and organic acids on treatment effectiveness. (Anderson and Benjamin 1985; Benali et al. 2001; Furukawa et al. 2002; U.S.EPA 2002; Liu and Huang 2003; Mladenov et al. 2009)

In this thesis, the citrate effect on arsenic removal efficiency in water treatment plants was examined and mechanisms of the citrate effect were proposed. One traditional

arsenic removal method (Ferric salt precipitation/coagulation) and one promising method (nanomagnitite adsorption) were applied to investigate the citrate influence comparably. With a focus on direct application, all the experiments were done at low molar ratios of citrate to iron, which has been rarely reported before.

1.1   Organization of Thesis

This thesis is organized into six sections. Following a brief introduction in section 1, background information and previous relevant research are reviewed in section 2. Materials and methods used in this study are described in section 3, results are presented and discussed in section 4, and major finding and future work are summarized in section 5.

2 Background and Literature Review

2.1 Arsenic Problem and Treatment

2.1.1 Sources and Occurrence

Arsenic (As) is a naturally occurring but not abundant semi-metallic element. It is present in over 200 minerals including arsenopyrite, niccolite, cobaltite, tennantite and enargite. Natural occurrence is the largest source of arsenic in the environment, while metal mining, fossil fuel combustion, and pesticides are also important anthropogenic sources. The earliest documented used arsenical copper as a poison was in 4000 B.C. by a Greek writer. Regardless of its high toxicity, arsenic is commonly used as pesticides and herbicides in wood preservation and agriculture, and also as a chemical warfare agent.

2.1.2 Fate and Transport in Environment

Arsenic can be mobilized and concentrated through both natural and anthropogenic activity. Arsenic ranks 52 among the element in the earth's crust with an average crustal concentration of 1.8 mg/kg. Arsenic background levels in different environmental media are listed in Table 1.

Environmental Media		Arsenic Level[*]
Atmosphere	Rural areas	0.02-4 ng/m^3
	Urban areas	3-200 ng/m^3
Hydrosphere	Ocean	1-2 µg/L
	Surface water	<10 µg/L
	Ground water [†]	1-2 µg/L
Geosphere	Sediment	5-3000 mg/kg
	Soil	1-40 mg/kg
Biosphere	Marine Organisms	<1~>100 mg/kg

Table 1 Arsenic background levels in the earth (Gomez-Caminero et al. 2001).

[*] Arsenic concentrations listed are background levels and exclude seriously contaminated scenarios.

[†] Arsenic levels can reach 3 mg/L in areas with volcanic rock and sulfide mineral deposits.

Geogenic processing of crustal materials to soil and groundwater is the primary natural pathway of arsenic into the geoshpere and hydrosphere. The dominant arsenic oxidation states are arsine (–III), arsenic (0), arsenite (+III), and arsenate (+V). Arsenite and arsenate are dominant natural species. Due to the double bond oxygen in the arsenate molecule (Table 2), arsenate has a greater dissociation constant, and mostly exists in an immobilized state by adsorption reactions with clays, natural organic matter, iron/aluminum/manganese oxides. However, arsenic is labile and readily changes oxidation state and chemical form with surrounding pH and redox potential (Figure 1). Therefore, once arsenate is absorbed to soil and is transported to groundwater that is reducing, it becomes more soluble and reduced state from arsenate to arsenite under normal pH conditions (Vance 1995; Frankenberger 2001; McArthur et al. 2001; Smedley

and Kinniburgh 2002). With the change of geological conditions, arsenic can be concentrated in soils to a typical range of 2-20 mg/kg and in groundwater to a range of 1-50 μg/L (Gomez-Caminero et al. 2001).

Volcanic action followed by low temperature volatilization contributes one third of the atmospheric flux of arsenic. Combustion of fossil fuels at high temperature also plays an important role in bringing arsenic into the atmosphere. In the atmosphere, arsenic occures almost exclusively as As_2O_3, adsorbed on particulate matter (Gomez-Caminero et al. 2001). However, arsenic can exist in the biosphere mostly in its organic form (Crecelius 1977). Inorganic arsenic and its compounds can be metabolized to a less toxic form by biological methylation (Bentley and Chasteen 2002). Seafood can contain up to 100 mg/kg of arsenic, although most food products contain less than 250 μg/kg. Nontoxic organic arsenic, arsenobetaine, has been found in some marine species consumed as food.
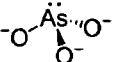
		pK_1	pK_2	pK_3
Arsenate		2.20	6.98	11.60
Arsenite		9.20	14.22	19.22

Table 2 Dissociation constants of arsenate and arsenite (pK_a).
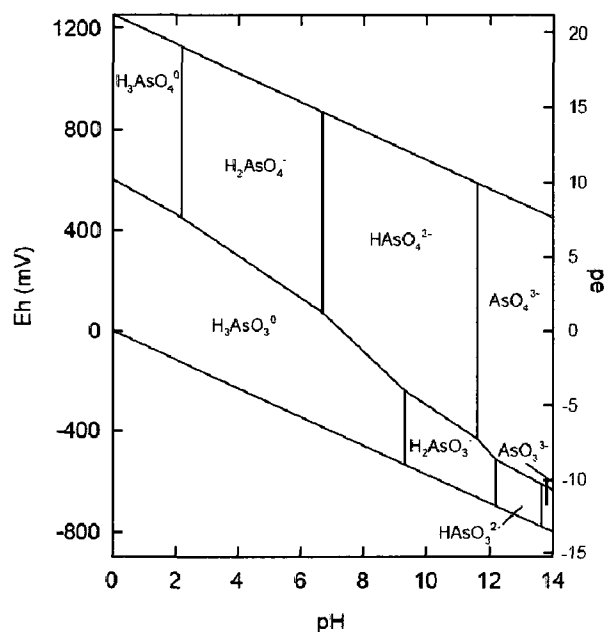
Figure 1 Eh-pH diagram of aqueous arsenic species in the system $As-O_2-H_2O$ at 25°C and 1 bar total pressure

(Smedley and Kinniburgh 2002).

2.1.3 Distribution in US and the world

The main regions of the world with arsenic problems include the scale of chronic human exposure and the four main sources (aquifer, geothermal, mining, and coal) of arsenic are depicted in Figure 2. Among 35 places identified in the map, 16 areas are contaminated by mining and 17 areas by geological contamination of aquifers. Geothermal sources are shown in three areas. Only Guizhou, China has serious arsenic contamination from burning coal. However, natural geological aquifers are the dominant source of arsenic for population at risk greater than 200,000. (Garelick and Jones 2008)

Arsenic distribution in ground water in the U.S. shows regional patterns of high concentrations in the West, and parts of the Midwest and Northeast but low concentrations in the Southeast (Figure 3) (Focazio et al. 2000). Among small drinking

ground water supply systems nationwide that serve between 1,000 and 10,000 persons, 10% have been estimated to exceed 10 µg/L (Figure 4) (Helsel 2000).
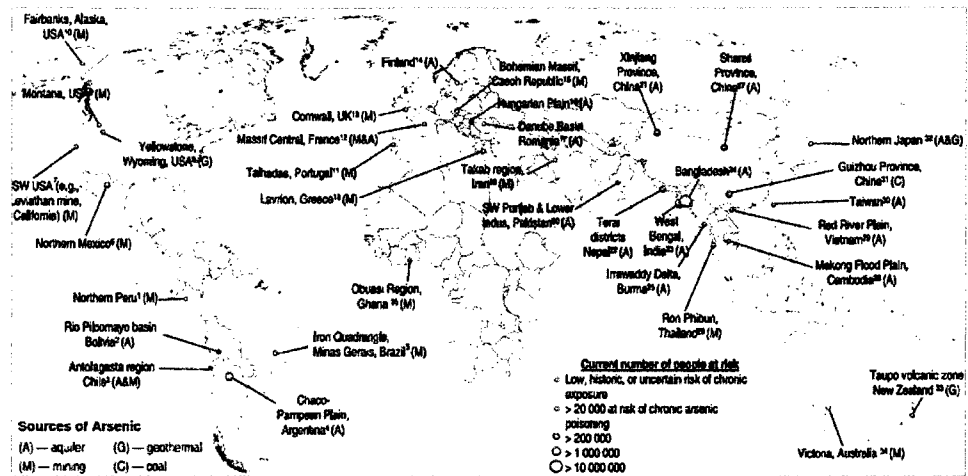
Figure 2 Worldwide distribution of arsenic contamination with source of arsenic and numbers of people at risk of chronic exposure (Garelick and Jones 2008).
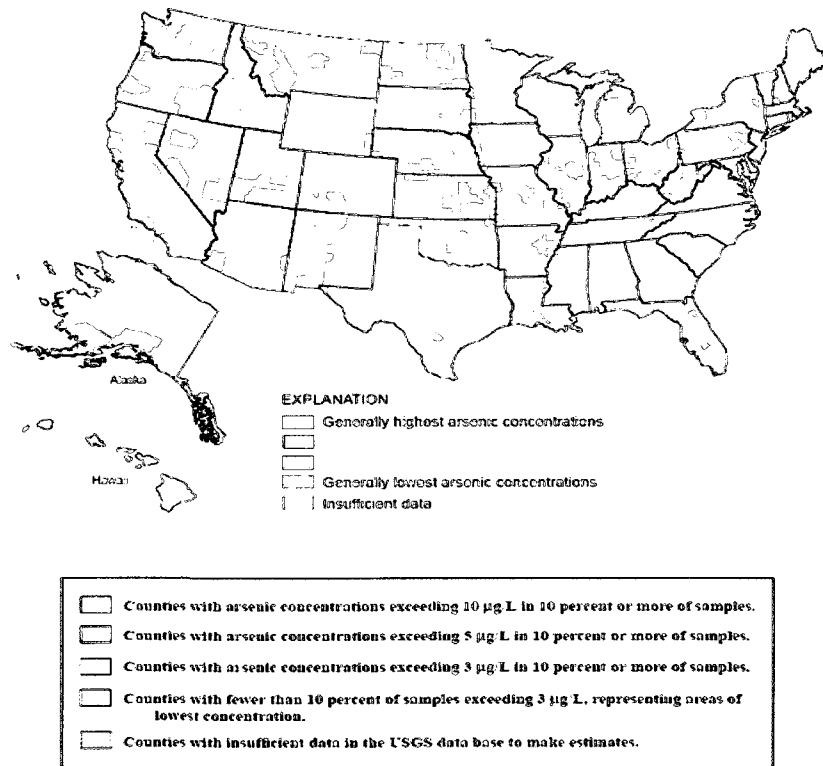
Figure 3 Counties with arsenic concentration exceeding target level in 10 percent or more of ground water samples from USGS data base (Focazio et al. 2000).
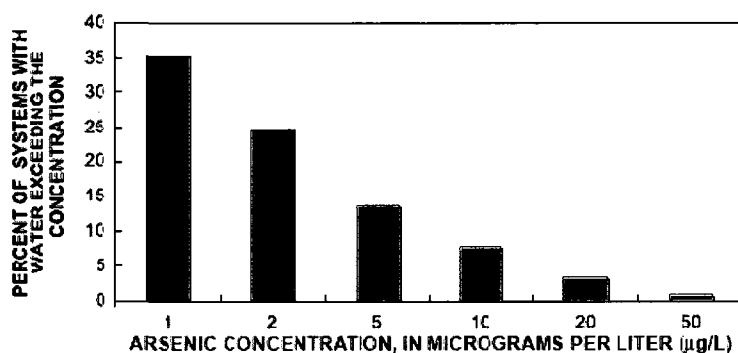
Figure 4 Percentage of small public water-supply systems estimated to exceed different level of arsenic concentrations

(Helsel 2000).

2.1.4 Health Effects and Regulation

Non-occupational human exposure to arsenic is mostly from ingestion of water as food and contaminated soils. The average intake of both inorganic and organic arsenic from food and beverage is 20-300 µg/day (Rasmussen and Andersen 2000). Arsenic metabolism has two main steps: reduction and methylation. First, arsenate (+V) is reduced to arsenite (+III). Then, arsenate is methylated to mono-, di-, and trimethylated products. The concentration of metabolites of inorganic arsenic in urine generally ranges from 5 to 20 ug/L (Crecelius 1977; Gomez-Caminero et al. 2001).

Different arsenic species show large variations in toxicity. Soluble inorganic arsenic is acutely toxic while organic species are almost non-toxic.(Crecelius 1977; Rasmussen and Andersen 2000; Garelick and Jones 2008) Once taken up by the human body, As (+III) is more extensively methylated but less toxic than As V. Arsenic is toxic by affecting NAD+ production, mitochondrial respiration and ATP synthesis (Thomas et al. 2007; Xu et al. 2008; Lievremont et al. 2009; Thomas et al.). Arsenic rich drinking

water is the main cause of chronic exposure to arsenic worldwide. Cancers of the skin, lungs, bladder and kidney, blackfoot disease, and skin changes have been reported from different arsenic contaminated areas (Rasmussen and Andersen 2000; Mandal and Suzuki 2002; Wilson 2009). Ingestion of large dose of arsenic can cause gastrointestinal symptoms, disturbances of the cardiovascular and nervous systems and eventually death. Bone marrow depression, haemolysis, hepatomegaly and other side effect symptoms have been observed in survivors of acute arsenic poisoning. High lung cancer risk was related to occupational exposure to arsenic primarily by inhalation (Saha et al. 1999; Gomez-Caminero et al. 2001).

Arsenic contamination did not draw public attention until the arsenic milk poisoning accident that occurred in western Japan in 1955. People suffered from after-effects of the poisoned milk 15 years after the accident.(Ui 1992; Mandal and Suzuki 2002) However, geological arsenic in aquifers was indentified to be the No. 1 source for arsenic exposure in Bangladesh (India). When the United Nations Children's Fund (UNicef) made an effort to predict the effect of water quality and supply on morbidity and mortality of children under five, it was unexpectedly discovered that 40 million people in Bangladesh were exposed to arsenic at toxic levels during the years 1980-1996 (UNicef 1998; Unicef 2008). Bangladesh is now regarded as the largest case of mass poisoning in recent history (Harvey et al. 2002; Chen and Ahsan 2004). A worldwide arsenic survey has identified several other countries as arsenic contamination areas, including China, the U.S. and as well as South America.(Chiou et al. 1995; Del Razo et al. 2002)

The World Health Organization (WHO) guideline value for arsenic is now 10 ug/L. Most developing countries still maintain the 50 ug/L standard first established in 1942. On October 31, 2001, based on the best available science and knowledge of arsenic toxicity and water treatment technology, as well as growing concerns on arsenic contamination, the U. S. Environmental Protection Agency (EPA) lowered the arsenic maximum contaminant limit (MCL) from 50 ug/L to 10 μg/L and set a goal of zero contamination. It has been four years scince this new standard went into effect on January 23, 2006 (Sombo 2000).

2.1.5 Arsenic Water Treatment Technologies

National Committee of Experts (NCE) identified four technologies as emergency responses to the arsenic crisis: pond-sand filters, dug wells, deep hand tube wells, and rainwater harvesting (Howard 2003). Arsenic removal technologies are not included in the list; however, those are discussed and developed in numerous research and field studies since those technologies are promising long-term and low-cost arsenic treatment for both surface and groundwater (Garelick et al. 2005). Five applicable technologies have been reported by U.S. EPA as recommended methods for arsenic water treatment. They are:

- Precipitation/coagulation and sedimentation
- Membrane filtration
- Adsorption treatment
- Ion exchange
- Permeable reactive barriers

Precipitation/Coagulation and sedimentation is the most frequently used large-scale technology with high removal efficiency and low capital investment and operation/maintenance (OM) cost to treat arsenic-rich water (Table 3). 45 full-scale and 24 pilot-scale applications of this low-cost and point-of-use technology have been reported in America (U.S.EPA 2002). Traditionally, precipitation transforms dissolved contaminants into an insoluble solid via a chemical reaction, while coagulation applies to the removal of contaminant (dissolved, colloidal or suspended form) adsorbed onto other particles. However, in all the studies of arsenic treatment technologies, precipitation emphasizes the process that takes the advantage of naturally occurring soluble iron in water. On the other hand, coagulation implies the introduction of a chemical coagulant (i.e. ferric chloride, ammonium sulfate) that absorbs arsenic and is finally removed from water by sedimentation or filtration. The processes of floc formation, particle aggregation and stabilization have all been covered in previous research on coagulation (Ahmed 2001; U.S.EPA 2002; El Samrani et al. 2006).

Ferric salt is considered as the most traditional and effective coagulant. Iron coagulation optimally removes over 95% arsenic at pH 5-8 with dosages between 2-25 mg/L (Sorg and Logsdon 1978; Edwards 1994; McNeill and Edwards 1995; McNeill and Edwards; Violante et al. 2007). Once ferric ions appear in aqueous solution, hydrous ferric oxide (HFO) is formed during hydrolysis. HFO has an extremely high surface area ($600m^2/g$) and high affinity for arsenic (Edwards 1994; Hering et al. 1997; Dixit and Hering 2003). However, HFO is thermodynamically unstable. It undergoes transformation to eventually form goethite. HFO can also be stabilized through anion

adsorption including phosphate, dissolved silicon, and organic acids (Betts 2001; Lytle et al. 2004; Violante et al. 2009).

Adsorption treatment is promising for small-scale, especially household treatment facilities, based on the growing body of knowledge in artificial nano particles. Nano magnetite has been reported to show a high capacity for arsenic adsorption and separation with high surface areas circa 100 m^2/g and low magnetic field gradients. An enhanced sand filter with commercial nano magnetite incorporated has been applied in a pilot field study in Guanajuato, Mexico (Yavuz et al. 2006; Farrell 2009; Shipley et al. 2009). Membrane filtration (reverse osmosis and nano filtration), ion exchange and permeable reactive barriers are also suitable at pilot-scale but require higher remediation budget by one order of magnitude and experienced operators (Vance 1995; U.S.EPA 2002).

	Technology	Removal Efficiency
Precipitaion/Coagulation	Iron salt	95%
	Aluminum	90% $As_{effluent}$=30 ppb
	Lime Softening	90%
	Bucket of Tea bag Method	80%-99% $As_{effluent}$=50-70 ppb
Adsorption	Activated Alumina	<50 ppb
	Nano Magnetite filter	$As_{effluent}$=0 ppb
	Iron filling sand	$As_{effluent}$<27 ppb
Ion Exchange		$As_{effluent}$<2 ppb
Membrane	Reverse Osmosis	86%
	Electrodialysis	80%
	Coagulation+Microfiltration	$As_{effluent}$<2 ppb
Permeable reactive barriers	Zero valence Iron filling	>94%-99%
Photo Oxidation		$As_{effluent}$=0 ppb

Table 3 Removal Efficiency and Cost of Available Arsenic Treatment Technologies (U.S.EPA 2000; Yavuz et al. 2006; Farrell 2009; Shipley et al. 2009).

2.2 Nano-crystalline Ferric Oxide Formation and Non-crystalline precursors

Ferric oxides are widespread. They are effective sorbents for a number of natural and anthropogenic dissolved ions (i.e. heavy metals) in water and gases since they often form fine crystals. Iron (III) oxides form by iron (III) reacting with OH⁻ in different structures. There are at least five polymorphs of FeOOH (α-FeOOH,β-FeOOH,γ-FeOOH,δ-FeOOH and ferrihydrite) and four of Fe_2O_3 (α-Fe_2O_3, γ-Fe_2O_3, Fe_3O_4 and Green rust), which can direct precipitate from Fe (II) Fe (III)solutions at various pH and temperature or transform from one iron oxide precursor by dissolution, reprecipitation or internal rearrangement within the structure (Figure 5). Two poorly crystalline structures are discussed here, ferrihydrite and akaganeite.
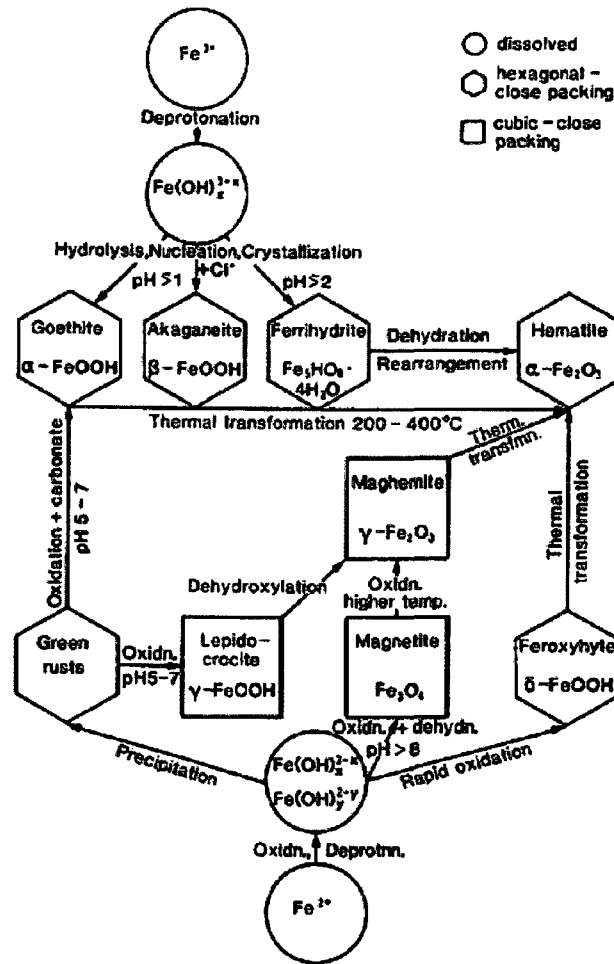
Figure 5 Schematic of major formation and transformation pathways of common iron oxides (Cornell and Schwertmann 2003).

2.2.1 Nano-crystalline Ferric Oxide

Ferrihydrite is poorly crystalline and an important precursor of more stable and crystalline ferric oxides. It was first reported by Chuckrov et al. in 1973 (Chuckrov and Zvyagin 1973). The precise structure of ferrihydrite is still not well known, because it resists traditional structure determinations and crystallographic methods, although $Fe_5O_8H \cdot H_2O$ is often used as a preliminary formula and two kinds of ferrihydrite (2-lines,

6-lines) with different X-ray diffraction (XRD) patterns are recognized (Figure 6) (Schwertmann et al. 1999; Schwertmann and Cornell 2000; Michel et al. 2007). A multiphase model for ferrihydrite containing three components: major defect-free crystallites (f-phase) (Figure 7) and two defective crystallites (d-phase and p-phase) have been proposed and observed (Drits et al. 1993; Janney et al. 2000; Janney et al. 2000). However, an ideal Fe_{13} Keggin structure of ferrihydrite was presented recently, which is the δ-isomer of Al_{13}-Keggin structure and will be discussed more in the Polyoxmelates section (Figure 8) (Michel et al. 2007; Penn 2007; Manceau 2009; Michel et al. 2010).
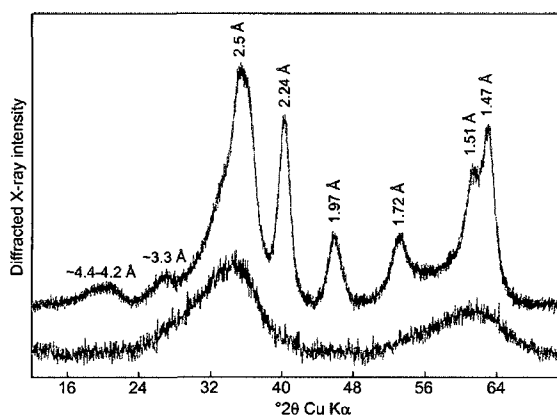
Figure 6 X-ray diffraction patterns for six-line (top lines) and two-line (bottom lines) ferrihydrite (Drits et al. 1993).

Akaganeite is named after the Akagane mine in Japan where it was discovered. It has been found all over the world and also in rocks from the Moon. Akaganeite formation requires the presence of chloride or fluoride ions. Structurally, Akaganeite has a body-centered cubic array rather than hexagonal close packing (hcp) or cubic close packing (ccp), occurring in all other iron oxides. There is a square tunnel housing the chloride ion by double chains of octahedral sharing corners with adjacent chains (Figure 8).

Schwertmannite $(Fe_8O_8(OH)_x(SO_4)_y)$, a mineral first described in 1994, is isostructural to akaganeite with sulfate in the middle of tunnels. Analogous structures were also indentified if selenate or chromate replace sulfate (Bigham et al. 1994; Bigham et al. 1996)
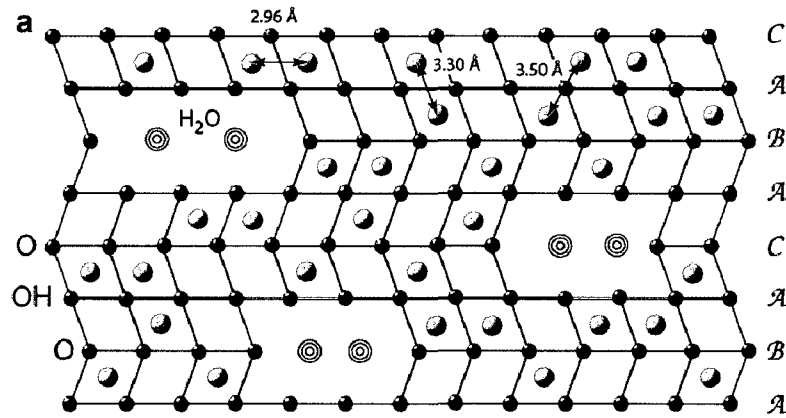
Figure 7 Projection of the defect-free component structure of ferrihydrite (f-phase) Iron, oxygen atoms are shown in yellow and blue, and water are shown in a black circle dispersed in the middle of oxygen atoms

(Drits et al. 1993).
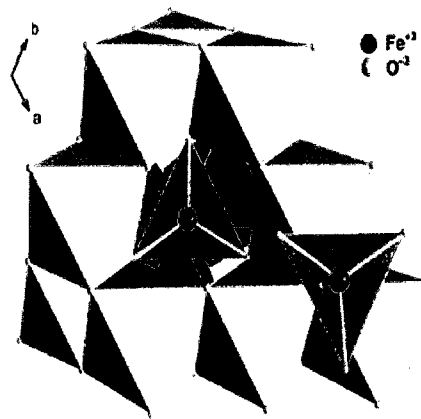
Figure 8 Fe_{13} Keggin structural proposed for ferrihydrite (Michel et al. 2007; Manceau 2009).
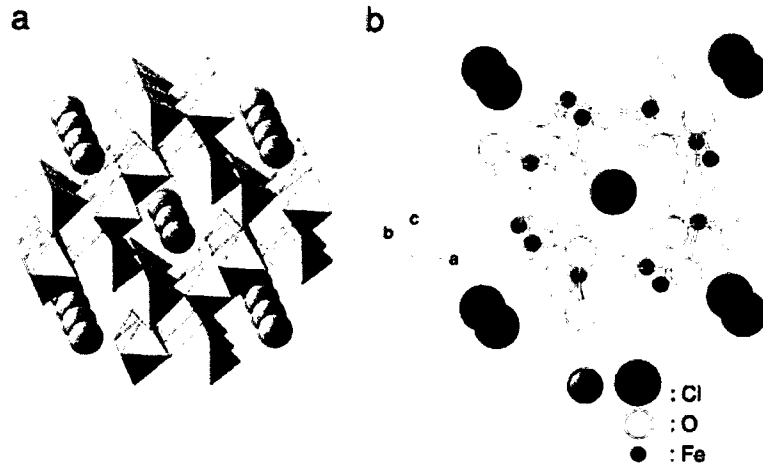
Figure 8 Akaganeite local structure a) Arrangement of octahedral double chains in tunnels with chloride ions in the centre of the tunnels b) Ball-and-stick model with unit cell outlined. (Cornell and Schwertmann 2003).

2.2.2 Non-crystalline Processors

In the presence of water, iron salts dissociate to form Fe^{3+} and force H_2O ligands to act as acid (Eq 1) followed by hydrolysis, step-wise deprotonation (Eq2 and Eq 3).

$$FeCl_3 + 6H_2O \leftrightarrow Fe(H_2O)_6^{3+} + 3Cl^- \qquad \text{Equation 1}$$

$$Fe^{3+} + H_2O \leftrightarrow FeOH^{2+} + H^+ \qquad \text{Equation 2}$$

$$FeOH^{2+} + H_2O \leftrightarrow Fe(OH)_2^+ + H^+ \qquad \text{Equation 3}$$
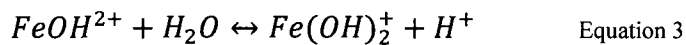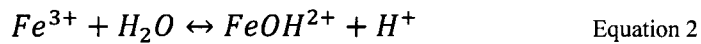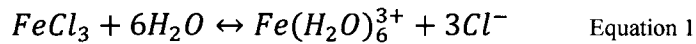
Hydrolysis of Fe corresponds to the formation of Ferric hydroxide and is often promoted by adding base, heating, dilution or high ionic strength. However, the pathways from soluble aqueous Fe (III) ions to various ferric hydroxides involve intermediate products. Studies on ferric hydroxides formation process are reported with various molar ratios of hydroxide to Fe (III), r=OH⁻/Fe(III). Monomer and dimer of ferric hydroxides exist in $Fe(NO_3)_3$ solutions up to r=0.5 (Cornell and Schwertmann 2003) before ferric nitrate polymer form. In $FeCl_3$ solutions at r<1.5, dimers ($Fe_2(OH)_4^{4+}$) with edge-sharing

octahedra form, followed by edge and corner-sharing trimers; while at r>=1.5, a condensed akaganeite-like Fe_{24} polycations formed by oxo bridges with a tunnel housing chloride in the middle. (Flynn 1984; Van der Woude et al. 1984; Bottero et al. 1994; Rose et al. 1997; Rose and Waite 2003).

2.2.3 Citrate effect

There are 792 registered products containing citric acid as an inert ingredient (4.5%-66%). EPA repealed the regulation of citrate in 2008, as citrate is generally recognized as safe (GRAS) (U.S.EPA 2008). Shanbrom suggested applying citrate-enhanced iodine treatment to destroy waterborne pathogens in drinking water (Shanbrom 2005). Yan presented a nitrate removal method from drinking water by adding sodium citrate as sole carbon source (Yan et al. 2005).

Citric acid is considered an excellent binder of a number of essential metal ions. Citrate retards the oxidation of Fe^{2+} and hinders goethite in favor of lepidocrocite at low molar ratios of citrate to Fe, but in favor of ferrihydrite at higher citrate to iron ratios. The formation and influence of an Fe-citrate complex was confirmed by crystallization, heavy metal removal and biological application (Spiro and Saltman 1969; Martin 1986; McGregor and H. 1992; Buerge and Hug 1998; Konigsberger et al. 2000). However, because of different preparation conditions (iron concentration, citrate/Fe molar ratio, pH, temperature) among individual studies, disagreements are found regarding as the predominate species of iron citrate complexes in solution (Table 4). At high molar ratios of citrate to iron (>10), a model consisting of $FeCit^0$, $FeCitH^+$, $FeCitH_{-1}^-$ and $FeCit_2^{3-}$ has been proposed to describe the Fe(III)-citrate system (Figure 8), and $FeCit^-$ and $FeCit_2^{n-}$

was reported to be the dominate species at pH 5-7 (Martin 1986; Konigsberger et al. 2000). The Fe_2Cit_2 complex was detected and characterized when molar ratios of citrate to iron fell to a range from 2.0 to 6.0, which is similar to the citrate/iron molar ratios under physiological conditions (Figure 9). This dimer complex was also extracted from iron transport system of *E. coli*. (Konigsberger et al. 2000; Ferguson et al. 2002; Hamada et al. 2003; Isabelle et al. 2005; Hamada et al. 2006; Evans et al. 2008). Shweky synthesized two dinuclear iron citrate complexes with using pyridine at physiplogical pH (Shweky et al. 1994).

However, Cornell and Schwertmann showed that citrate, at low concentrations, effectively inhibited the conversion of ferrihydrite to goethite (Cornell and Schwertmann 1979; Ferguson et al. 2002). Krishnamurti and Huang observed that a strong non-crystal iron complex formed at a citrate/Fe molar ratio of 0.1 and inhibited iron crystallization (Krishnamurti and Huang 1991). Moreover, Spiro isolated a macromolecular fraction with composition $Na_5[Fe_{20}O_{20}(OH)_{13}Cit_3]$ by membrane filtration and demonstrated that excess citrate prevented the formation of this macromolecular (Spiro et al. 1967).

Ionic Strength	pH	Temperature (°C)	[Fe]$_0$* (M)	Maximum Molar Ratio(Citrate/Fe)	Ferric Citrate Complex	Ref.#
0.01M	5	13-31	1×10^{-2}	16.7	N/A	(Buerge and Hug 1998)
0	7.4	N/A	1×10^{-5}	10.0	$(FeCitH^{4-})_2$	(Hamada et al. 2006)
1.0M	1.3-5.4 ※	25	9.7×10^{-3}	2.6	$Fe_2Cit_2OH^{5-}/Fe_2Cit_2H_4{}^{4+}$	(Konigsberger et al. 2000)
0	8-9	N/A	1×10^{-3}	1.0	$Na_5[Fe_{20}O_{20}(OH)_{13}Cit_3]$	(Spiro et al. 1967)
1.25M	9 – 11	70	4.75×10^{-2}	0.2	N/A	(Cornell and Schwertmann 1979)
0	6	23.5	1×10^{-2}	0.1	N/A	(Krishnamurti and Huang 1991)
0.01M	8	25,45	9×10^{-5}	0.28		This study

* [Fe]$_0$ refers to an initial total iron (III) concentration.

※Titrations were done in this research.

Table 4 Experimental conditions of the Fe-Cit system: present study vs that in literature.
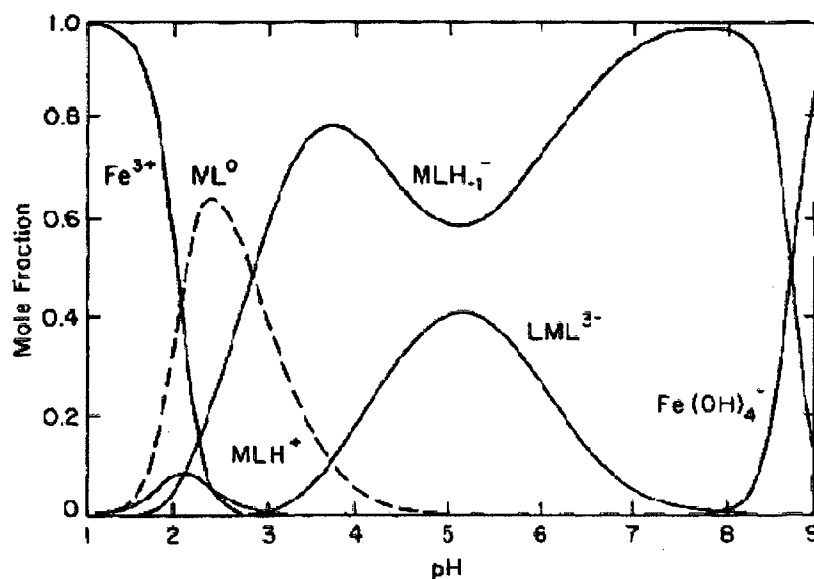
Figure 9 Species distribution for 1 μM Fe^{3+} and 0.1 mM citrate plotted as mole fraction vs pH. MLH$_{-1}{}^-$ indicates the deprotonated species (Martin 1986).
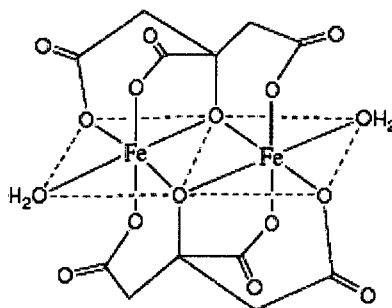
Figure 10 Structure of Fe_2Cit_2 complex (Evans et al. 2008).

Added anions may also affect the purity of the crystal by forming different precursors. Strong structural binding effect was found with various anions. Chloride and other halogenides hinder the formation of Fe-O-Fe linkages. Chloride, sulfate and carbonate will stabilize the green rust precursor by directing the spatial arrangement of double chains of $FeO_3(OH)_3$ octahedra to FeOOH forms. Silicate promotes the formation of ferrihydrite rather than lepidocrocite. Phosphate suppresses goethite in favor of lepidocrocite (Benali et al. 2001).

2.3 Supramolecular and Polyoxometalates

2.3.1 Background

Inspired by Richard Feynman's first speech about nanotechnology, entitled "There's plenty of room at bottom", at the 1959 meeting of the American Physical Society at Caltech, modern molecular chemists have developed method to directly manipulate and control individual atoms, a powerful synthetic chemistry method to construct large molecules (Feynman 1960). This coined "bottom up" approach has been widely developed in materials science and biological applications.

Supramolecular chemistry refers to the chemistry beyond the molecule, which investigates the molecular assemblies and intermolecular (noncovalent) bond (Steed and Atwood 2000). Supramolecule is generally considered as the product of a molecule (a host) and another molecule (a guest) complex. Normally, the host is a large molecule or aggregate (i.e. enzyme, synthetic cyclic compound) providing a sizeable central hole or cavity, while the guest may be a monatomic cation, a simple inorganic anion or a more complicated molecule. Supramolecular complexes are combined by ion pairing, by metal to ligand binding, by hydrogen bonding, by van der Vaals interaction, by π-π interaction, etc (Cram and Cram 1994).

With a diverse range of molecular clusters, supramolecular clasters show ability to form structures that can bridge several length scales and it is considered as a missing link between the "bottom up" approach and the traditional "top down" approach (Cragg 2005). The unique structure formed by electrostatic forces rather than covalent bonds between a host and a guest is a fascinating subject in recent chemistry research and dramatically inspire the developing of nanoworld.

As a branch of supramolecules, polyoxometalates (POM) refer to a polyatomic ion, usually consists of three or more early transition metaloxyanions linked together by sharing oxygen atoms. There are three classes of POM structure: 1) Isopolyanions with only metal-oxide framework; 2) Heteropolyanions, with hetero anion (PO_4, SO_4) inside the metal-oxide framework; 3) Mo-blue $\{Mo_{154}\}$ POM clusters (Figure 11) (Long et al. 2007).

The interest of polyoxometalates dates back to the 19th century when Berzelius reported 12:1 composition, which is now known as $(NH_4)_3[PMo_{12}O_{40}]_{aq}$ (Berzelius 18).

The structure of this 12:1 heteropoly species was not defined until Keggin came up with a hexahydrate composition $(H_5O_2)_3[PW_{12}O_{40}]$ in 1933 (Keggin 1933). Polyoxometaltes chemistry emerged in the middle of 20th century, when scientist reported hundreds of polyanions. Souchay was their vanguard in the study of condensation reactions of molybdate and tungstate in solution by extensively using polarography techniques. The discovery of "magic building block" ability of $[Mo_2S_2(H_2O)_6]^{2+}$ precursor for the design of cyclic structures promoted the development of supramolecular chemistry (Gouzerh and Che 2006). During the last 15 years, the mystery of molybdenum blue has been uncovered by Muller in 1995 with the discovery of the Bielefeld giant wheel structure, $\{Mo_{154}\}$ crystallized from a Mo-blue solution. A spherical balllike $\{Mo_{132}\}$ structure was synthesized by changing the pH and incorporation of reducing agent to provide a more protonation condition and was referred to as the highly reduced POM. A large variety of clusters corresponding to different physical and chemical properties can be obtained by self-assembly with controlled conditions in the aqueous solution, which leads POM study to various applications (Muller 2003). For example the $\{(Mo)Mo_5\}_{12}\{FeIII\}_{30}$ formation by the reaction of Keggin anions $[PMo_{12}O_{40}]^{3-}$ with iron(III) ions incorporate magnetic properties to the original keggin structure by reforming a giant icosahedral cluster. Generally, POM can be produced by acidifying an aqueous solution containing the relevant metal oxide anions (molybdate, tungstate and vanadate) (Figure 12) (Pope and Muller 1991).

Some common POM structures in polyhedral representations

a) The $[M_6O_{19}]^{n-}$ "Lindqvist" structure (O_h symmetry) is a compact arrangement of six edge-shared MO_6 octahedra (known for M = Mo, W, Nb, Ta). b) The α-$[(XO_4)M_{12}O_{36}]^{n-}$ "Keggin" structure (T_d symmetry) is composed of four M_3O_{13} groups of three edge-shared MO_6 octahedra, linked by corner-sharing to each other and to the central XO_4 tetrahedron (M = Mo, W; X can be a non-metal, e.g. P^V and Si^{IV} or a metal, e.g. Co^{III} and Cu^I). c) The α-$[(XO_4)_2M_{18}O_{54}]^{n-}$ "Dawson" structure (maximum symmetry D_{3h}) is made by fusion of two A-α-XM_9O_{34} "Keggin" fragments (known for M = Mo, W; X = P, As, S). d) The $[H_x(XO_6)M_6O_{18}]^{n-}$ "Anderson" structure (D_{3d} symmetry) is a planar arrangement of seven edge-shared octahedra (e.g. X = I, M = Mo, x = O, n = 5; X = Cr, M = Mo, x = 6, n = 3]. e) The $[(XO_{12})M_{12}O_{30}]^{n-}$ structure (maximum symmetry I_h) may be viewed as a XO_{12} icosahedron surrounded by six equivalent M_2O_9 groups of face-shared MoO_6 octahedra, linked together by corner-sharing (known for M = Mo, X = tetravalent lanthanide and actinide cations).

Figure 11 Common POM structures in polyhedral representations (Gouzerh and Che 2006).
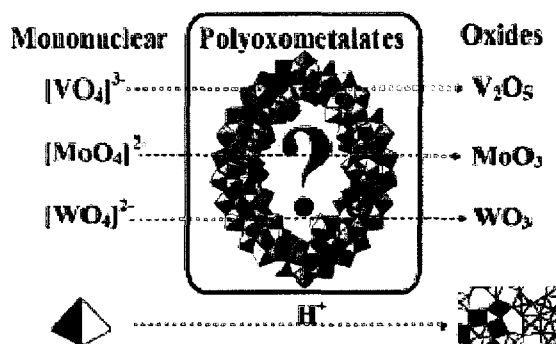
Figure 12 POM formation as long as the system is not directly driven to the oxide (Long et al. 2007).

2.3.2 Keggin Al_{13} and Fe_{13}

The Keggin structure is well-known as the most thermodynamically stable structure of polyoxometalate catalysts (Figure 13). The α-Keggin anions has a general formula $[XM_{12}O_{40}]^{n-}$. (X is the heteroatom, such as P^{5+}, M is the metal) The structure name is after J.F. Keggin who first experimentally determined the structure of α-Keggin anions (phosphotungstate) in 1934 (Keggin 1933). This structure can self assembles in

acidic aqueous solution and α-Keggin anions can be reversibly reduced by accepting electrons, which make them as good catalysts for organic reactions. Keggin structures consist of 12 octahedral MO_6 housing one heteroatom. There are 24 bridging oxygen atoms that link the 12M. The central heteroatom connects to 12M in four M_3O_{13} units by four oxygen atoms, giving an overall tetrahedral symmetry (Tianbo et al. 2004). There are 5 isomers of Keggin structures (α-,β-,γ-,δ-, ε-) by different rotational orientations of the M_3O_{13} units.
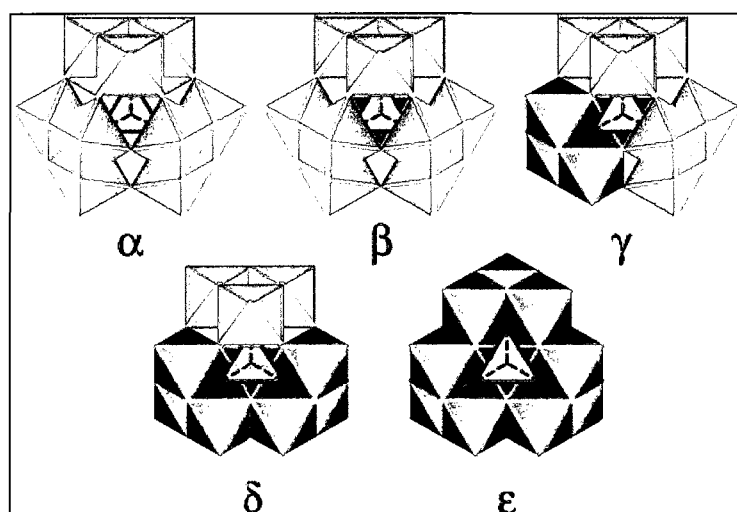
Figure 13 The Baker-Figgis-Keggin isomers shown in polyhedral representation.

The isomers are the stepwise rotation of trimeric groups of $Al(O)_6$ octahedra from corner-sharing (light gray) to edge-sharing (darker gray) (Casey 2005).

Thanks to the application of ^{27}Al nuclear magnetic resonance spectroscopy, the hydrolysis of $AlCl_3$ is well documented. Three major species during Al^{3+} hydrolysis have been determined: monomer $Al(H_2O)_6^{3+}$, dimer $Al_2(OH)_4^{4+}$, and "Al_{13}", $Al_{13}O_4(OH)_x^{(31-x)+}$ (Greenwood and Earnshaw 1997). Two classes of the latter large aqueous aluminum

hydroxide molecules were investigated. One has the Keggin structure with a central tetrahedral $Al(O)_4$ site α- Al_{13}, δ- Al_{13}, ε- Al_{13}, while the other one is a molecular clusters based on brucite-like $Al_3(OH)_4^{5+}$ cores, coined as "flat - Al_{13}". In water treatment plants, aluminum chlorohydrate is added to form cationic sols that adsorb metals and organic contaminates. Keggin ε-Al_{13} is stable for at least 12 years at ambient conditions but it can convert to Al_{30} over this time scale or at elevated temperatures. Natural ε-Al_{13} molecule was reported in a higher-pH solution rapidly mixed with acidic and low-organic acid waters, such as dilution of acid rainfall percolating through soil into a higher-pH stream or over a limestone terrain (Bottero et al. 1987; Furrer et al. 2002; Casey 2005).

An ideal Fe_{13}-δ-Keggin structure of ferrihydrite was presented by Michel et al, 2007. from simulation of the atomic pair distribution function (PDF) obtained by Fourier transformation of diffraction data, in the five decades since Johansson first isolated and crystallized the ε-Al_{13}. The structural motif of this new model is the δ-isomer of Al_{13}-Keggin structure and has one FeO_4 tetrahedra surrounded by 12 FeO_6. The similarity in the underlying structure of 2-line and 6-line ferrihydrite was reported in their previous work. (Figure 14) (Michel et al. 2007; Michel et al. 2007; Manceau 2009; Michel et al. 2009) Similar keggin 13 iron molecules were synthesized by adding ferric fluoride trihydrate and pyridine in hot methnol (Bino et al. 2002).
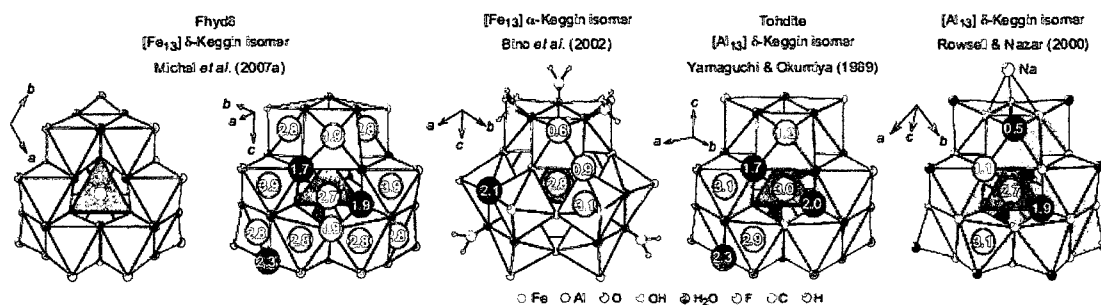
Figure 14 Proposed polyhedral representation of Fe_{13} and Al_{13} keggin structure (Manceau 2009)

2.3.3   Analytical method (ESI-MS)

Electrospray ionization mass spectrometry (ESI-MS) (Fenn et al. 1989; John 2003) is a newly developing analytical technology which acquires mass spectra directly from solution samples and has a detection limit as low as $10^{-6}M$. Incidentally, the powerful and elegant analysis performance of ESI-MS to the large and fragile polar molecules helped John Bennett Fenn earn the Nobel Prize in Chemistry in 2002. ESI is a soft ionization technology that produces intact ions from molecular species into an ambient bath gas (normally N_2) instead of traditional vacuum by applying sufficiently rapid energy input to lead to vaporization before decomposition (Dole et al. 1968; Beuhler et al. 1974; Whitehouse et al. 1985; Paul and Udo 2009).

Analyte dissolved in a volatile solvent flows into the eletrospray chamber through a stainless steel hypodermic needle, at whose tip a few kilovolts electrical field is applied and form a so-called Taylor cone (Figure 16 and Figure 17). The Taylor cone helps the liquid disperse into micrometer-sized charged droplets by Coulomb repulsion. A countercurrent flow of bath gas at 800 torr, an initial temperature from 320-350K, and a flow rate of 100m/s enhance the evaporation of organic solvent from each droplet of ever-decreasing diameter (Fenn 2000; Nguyen and Fenn 2007). Therefore, the surface charge of the droplet will increase until Coulomb repulsion raise to the same order of magnitude as the surface tension, resulting in Coulomb explosion. Coulomb explosion repeatedly tears droplets until it is small enough to lose ions from its surface into the ambient gas. Figure 16 and Figure 17 show the schematic view of ESI source and Coulomb explosion theory. The ions from small droplet are called quasi-molecular ions and suitable for mass spectrometric analysis. Two possible pathways (Figure 15) for ion

formation from a charged liquid droplet were presented by Dole in 1968 and Iribarne and Thomson in 1976. In the former model, the final ion is produced by desorption while the latter one by evaporation of surrounding solvent (Dole et al. 1968; Iribarne and Thomson 1976; Tomson and Iribarne 1979; Consta et al. 2003).
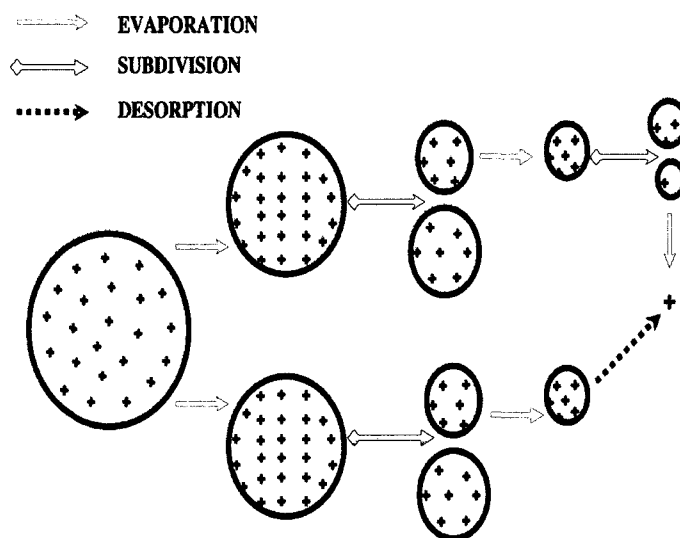
Figure 15 Schematic of the possible pathways for ion formation from a charged liquid droplet.

The upper is depicted by Dole's theory and the lower by Iribarne and Thomson theory (Nguyen and Fenn 2007).
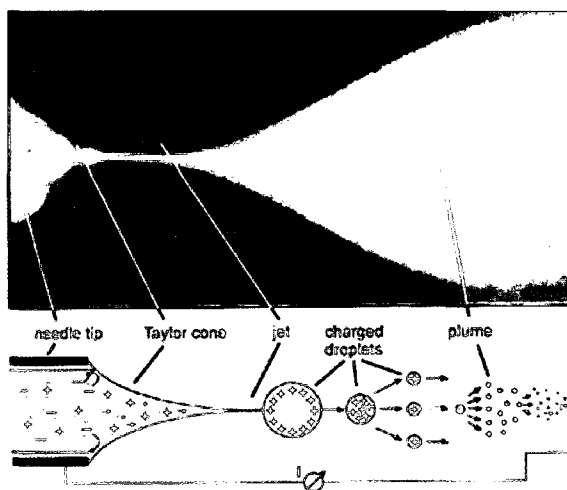
Figure 16 Photograph and a schematic picture of the spray in ESI source (Schalley 2007).
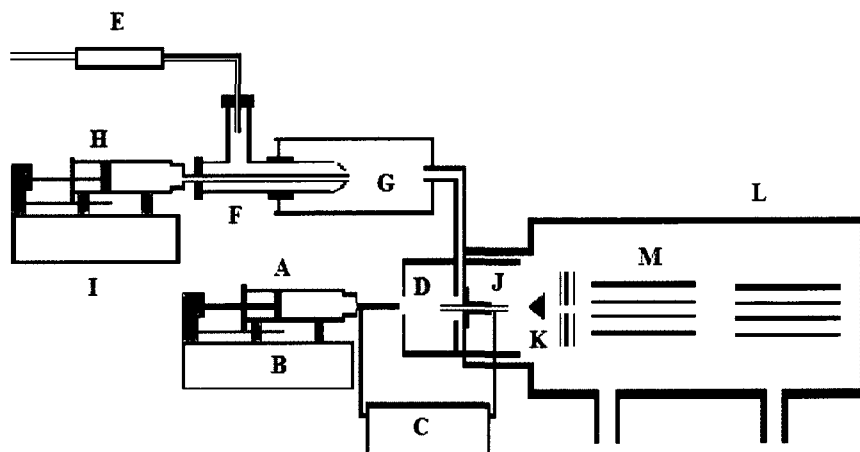
Figure 17 Schematic diagram of the apparatus contains essential components of the experimental system shown are a syringe containing analyte solution.

(A), a syringe pump (B), a high-voltage dc power supply (C), a vapor/bath gas chamber (D), a gas flow meter (E), a concentric nebulizer (F), a spray chamber (G), a solvent-containing syringe (H), a pump for delivering precise amounts of liquid solvent to the concentric nebulizer (I), a brass capillary (J), a conical skimmer (K), a vacuum chamber (L), and a quadrupole mass analyzer (M) (Nguyen and Fenn 2007).

Compared with potentiometric, spectrophotometric, calorimetric and other traditional complex measurement methods, ESI-MS has been provn to be very useful in the study of qualitatively confirmation of a complex in metal-ligand systems during the past 20 years. 19 studies were reported to give the number and stoichiometry of iron ligands species by using ESI-MS from Caudle's first try in 1994 (Caudle et al. 1994; Valerio and Bombi 2006). Gautier-Luneau observed trinuclear ferric citrate species by comparing the X-ray structures and solution species (Isabelle et al. 2005). Nischwitz confirmed metal citrates speciation at a molar ratio of 1:10 and developed ESI-SRM (selected reaction monitoring) method from ESI-MS to improve the selectivity and

sensitivity (Volker and Bernhard 2009). However, Neubert found no evidence for an iron

citrate complex in aqueous solution at pH 6.0 at a 1:2:10 molar ratio of Fe/3-hydroxy-2-

methyl-1-propyl-1H-pyridin-4-one/citrate (Hendrik et al. 2002).

3 Materials and Methods

3.1 Apparatus

All the nucleation kinetics and adsorption experiments were executed using an apparatus (Figure 18) consisting of a 500 mL water-jacketed ACE brand glass reactor and a 316 stainless steel lid sealed to the reactor with a O-ring. An overhead propeller agitator was installed through the central hole of the lid and allowed to rotate (Arrow Engineering, Hillside, NJ, USA) at about 180 rpm, changing direction every 5 seconds. 1/16" PEEK tubing was used for sampling and injection. Temperature of the reactor was maintained by refrigerated and heating circulator (Julabo East, Allentown, PA, USA).
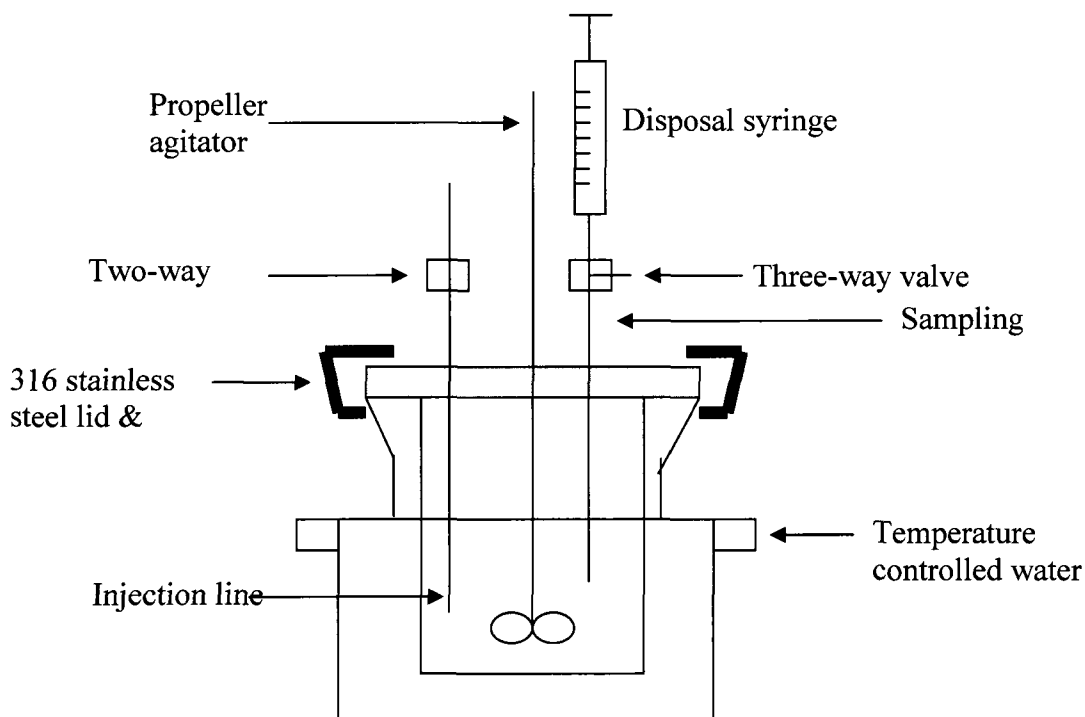
Figure 18 Apparatus setting for the ferric hydroxides nucleation and arsenate adsorption.

3.2 Materials

All chemical were analytical grade. Fe (III) stock solution was made by dissolving 909 mg $Fe(NO_3)_3 \cdot 9H_2O$ in 50 mL of deionized water. As (V) stock solution was made by dissolving 154mg $As_2O_5 \cdot 3H_2O$ in 100mL of deionized water. Electrolyte solution containing 0.01 M $NaNO_3$ and 0.001 M $NaHCO_3$ was used to simulate nature water system with IS of 0.01M, and seven stock solutions containing 0.05 M different carboxylic acids were prepared (Table 5).
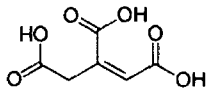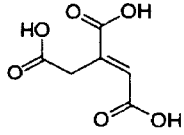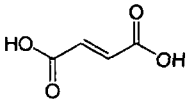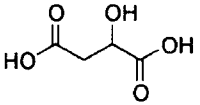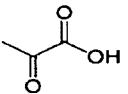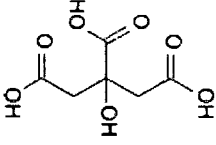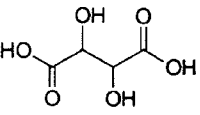
Carboxylic acid	Formula	Structure
cis-Aconitic acid	$C_6H_6O_6$	
trans-Aconitic acid	$C_6H_6O_6$	
Fumaric acid	$C_4H_4O_4$	
Malic acid	$C_4H_6O_5$	
Pyruvic acid	$C_3H_4O_3$	
Citric acid	$C_6H_8O_7$	
DL-tartaric acid	$C_4H_6O_6$	

Table 5 Formula and structure of eight carboxylic acids in this study.

3.2.1 HFO

2-line ferrihydroxide was prepared by modifying Schwertmann and Cornell's method (Schwertmann and Cornell 2000). A 0.1 M NaOH solution was added into a 90 μM solution of $Fe(NO_3)_3 \cdot 9H_2O$ with constant agitating until the pH reached 8.0.

3.2.2 Nano Magnetite

Commercially prepared magnetite nanoparticles from Reade Advanced Materials (Reno, NV, USA) were used (Figure 18). Characterization was reported in previous work (Shipley et al. 2009). Briefly, Brunauer-Emmett and-Teller (BET) surface area was 60 m^2/g, point of zero charge (pzc) ranges from 6.4 to 7.2, bulk density was 0.84 g/cm^3, true density was 4.8-5.1g/cm^3, nominal particle size was 19.3 nm.
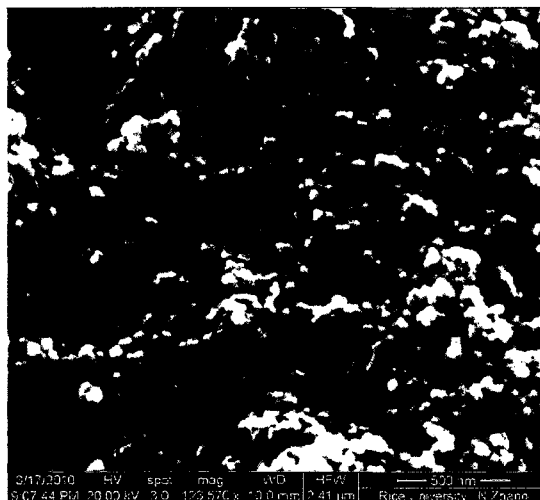
Figure 19 SEM image of Reade nanomagnetite.

3.3 Ferric Hydroxide Nucleation

Suitable amounts of carboxylic salt stock solution were added into 450 mL electrolyte in the reactor at 25°C. The Fe (III) stock solution was then added into the reactor. The pH was adjusted to 6.0, 7.0 and 8.0 respectively by 0.1 M NaOH. Carboxylic/TotFe (III) molar ratios range from 0.05 to 0.28. At selected time intervals, 5 mL aliquot suspensions were collected and filtered through a 0.45 μm Nalgene syringe Surfactant-Free Cellulose Acetate (SFCA) filter (Fisher scientific, Houston, TX, USA) using a disposable syringe. Then the filtered samples were acidified with 1% nitric acid for sample preservation prior to concentration analysis. For electrospray mass spectrometry experiments, the filtered samples were diluted with acetonitrile to 50% to assist solvent evaporation in the ion source. The ferric hydroxide nucleation, without carboxylic salt, was used as a control experiment in the whole study.

3.4 Arsenate Adsorption

Arsenic (V) adsorption on Ferric Hydroxide in the presence of sodium citrate was determined at pH 8 by the same procedure as for ferric hydroxide nucleation except 1.2 μM Arsenic was added to in the reactor.

Instead of ferric salt, 0.1 g/L of 20 nm magnetite was added in the reactor to investigate arsenic (V) adsorption on nano magnetite in the presence of sodium citrate was also investigated at pH 8.

3.5 Instrument analysis

3.5.1 Inductively coupled plasma-mass spectrometry (ICP-MS) and optical emission spectrometry (ICP-OES)

Total arsenate concentration in solution was measured using inductively coupled plasma-mass spectrometry (ICP-MS, Perkin Elmer Elan 9000, Atlanta, GA, USA). Total iron concentration was measured using inductively coupled plasma-optical emission spectrometry (ICP-OES, Perkin Elmer Optima 4000 DV, Atlanta, GA, USA). Detection limit of arsenic using ICP-MS is 5ng/L (6.7×10^{-5} μM) and detection limit of iron using ICP-OES is 0.01mg/L (0.18 μM). Instruments were calibrated, each time, before use. With four-point calibration, ICP-MS was calibrated from 0 to 1.35 μM with arsenic standard solutions, and ICP-OES was calibrated from 0 to 179 μM with iron standard solutions. Yttrium and germanium were used as an internal standards and a quality control sample was analyzed every six samples.

3.5.2 Dynamic Liquid Scattering (DLS)

Dynamic Liquid Scattering (Zeta Pals 90, Brookhaven Int. Co., Holtsville, NY, USA) was used to measure the size of ferric hydroxide suspension in the solution after 1hr reaction.

3.5.3 Eletrospray ionization mass spectrometry (ESI-MS)

All electrospay experiments were carried out with ESI-micoTOFMS (Bruker Daltonics, Billerica, MA, USA) in the 100-1000 m/z range (Figure 19). The instrument was operated in positive ion polarity mode employing the following conditions: capillary

voltage 4800 V; end plate offset -500 V; nebulizer gas (N_2) pressure 0.2 bar; dry heater temperature 180 °C; dry gas (N_2) flow 3.0 L/min. The sample was injected using a syringe pump at 5.0 μL/min.
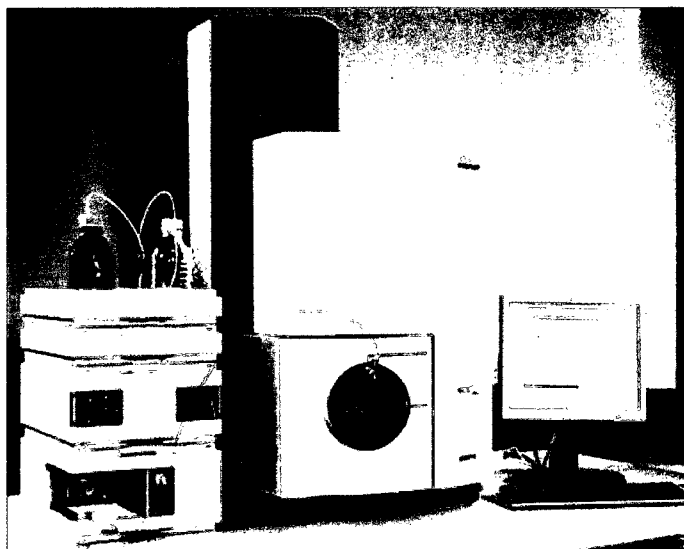
Figure 20 ESI- micrOTOFMS with TOF repetition rate up to 20 kHz.

3.6 Fe-Citrate complex molecular modeling

A Fe_4Cit complex was modeled using Density Functional Theory (DFT), a standard method for quantum chemical modeling of transition metals. All calculations were performed using Gaussian 03 software (Gaussian Inc, Pittsburgh, PA, USA) (Frisch 2003). The molecular geometry of $[Fe_4O_{13}H_4Cit]^{2+}$ was optimized by a chemistry model containing the Becke-Lee-Yang-Parr (BLYP) functional, and the LanL2DZ basis set for Fe, assuming C_{3h} symmetry. The perspective image of Fe_4Cit molecular structure was made by Visual Molecular Dynamics (VMD) software support. VMD was developed with NIH support by the Theoretical and Computational Biophysics group at the Beckman Institute, University of Illinois at Urbana-Champaign.

4 Results and Discussion

4.1 Effect of Citrate on Arsenic Removal

4.1.1 Negative effect on iron precipitation and coagulation method

Citric acid is commonly found in natural water in the concentration range of 10 to 1000 μM. 5-25 mg/L (90-450 μM) ferric salts are used to aid in removing particles and heavy metal ions in the water by precipitation and coagulation in water treatment plants. Therefore, the molar ratio (MR) of citrate to iron in water treatment plants is in the range from 0.02 to 10, which includes both high MRs and low MRs. The influence of citrate on heavy metal removal at low MRs (<1) has rarely been reported, although some work has been conducted at high MRs (>1) (Buerge and Hug 1998; El Samrani et al. 2006). In this study, MRs ranging from 0.03 to 0.28 were studied.

The effect of citrate on arsenic removal efficiency in Houston tap water with 1.2 μM arsenic (V) was evaluated with approximately 90 μM ferric iron as ferric nitrate ($Fe(NO_3)_3 \cdot 9H_2O$) at pH 8, with ionic strength at 0.01 M (Figure 20). Without citrate, a rapid reduction of arsenic concentration in solution occurs, and residual iron concentrations during the reaction are negligible. On the other hand, almost complete inhibition of arsenic removal occurs at citrate concentrations above 4.5 μM, which corresponds to the initial citrate to iron MR of 0.05, and higher (Figure 20). The arsenate concentration remains constant at about 95% of initial concentrations with the maximum deviation of 0.02 in C/C_0.

These results suggest that the presence of citrate, even at low molar ratios, can significantly affect arsenic removal. Citrate plays an important role on holding iron and

arsenic in the aqueous phase. Ferric hydroxide cluster and attached arsenic were stabilized in the solution and were prevented from further aggregating and precipitation. This stabilized colloid might contain Fe-Cit and Fe-As-Cit macromolecular complex. There would be no precipitation or coagulation, therefore, arsenic contamination retrains in the aqueous phase without removal.
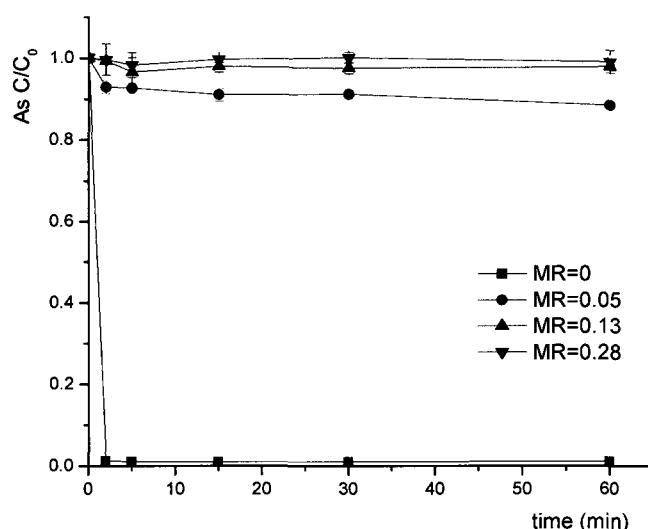
Figure 21 Arsenate removal efficiency vs. time in the presence of citrate and Fe (III) with various MR at pH=8 and

T=25°C.

4.1.2 Effect of citrate on magnetite absorption

Compared to the 100% removal seen with traditional iron salt coagulation, the efficiency of arsenate removal at 0.1g/L nano magnetite only reached 50% (Figure 21). It was expected that citrate would completely prevent magnetite from removing arsenate, but this didn't occur. Instead, the concentration of As smoothly dropped to 80% of the

initial value after 1 hour of reaction, at which point the adsorption of arsenic on nano magnetite hadn't reached equilibrium. The suppressed adsorption of arsenate may be because of the competition between citrate and arsenate for the active binding sites on the adsorbent (M. Grafe 2001; Grafe et al. 2002) However, the inhibition of arsenate removal happened in the presence of citrate, regardless of the citrate concentration which ranged from 1 to 5ppm. The amount of citrate used here is the same as in the other experiments in this study with ferric salts. The results show clearly that the active sites for arsenic adsorption aren't completely blocked by citrate, and the ability of arsenic adsorb onto nanomagetite doesn't change with increasing citrate concentration. Citrate may affect the arsenic removal not by combining with iron oxides, but by combining with arsenate. Arsenate can first complex with citric acid, and the subsequently added nano magnetite may absorb this new arsenate-citrate complex, but with lower affinity. The Fe-Cit complex and As-Cit complex may form simultaneously, but As-Cit apparently has much stronger affinity for the magnetite surface.

Ferric salts precipitation and coagulation is a traditional method in water treatment plants for heavy metal removal. Magnetite nanoparticles have been proven to be a very promising adsorbent for removing heavy metals from drinking water, especially for arsenic removal. The presence of citrate at low MRs (<1) in the solution has a much more significantly negative effect on arsenic removal by iron salt precipitation and coagulation methods than by magnetite adsorption (Figure 23).

Arsenic Removal Inhibition

Arsenic Removal	Ferric Salt	Magnetite
■ Arsenic removal without citrate	100%	50%
■ Maximum Arsenic removal with citrate	10%	20%
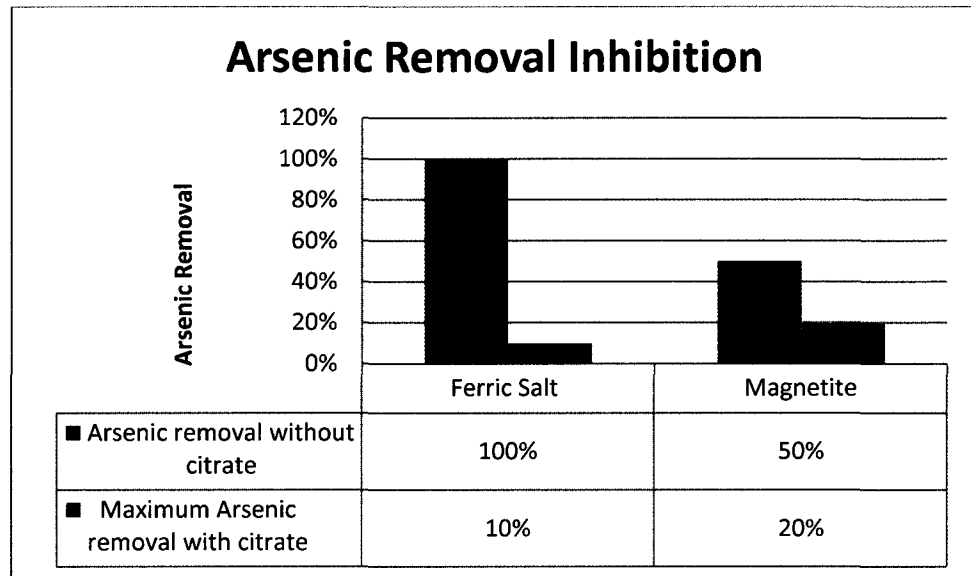
Figure 22 The effect of citrate on arsenic removal.
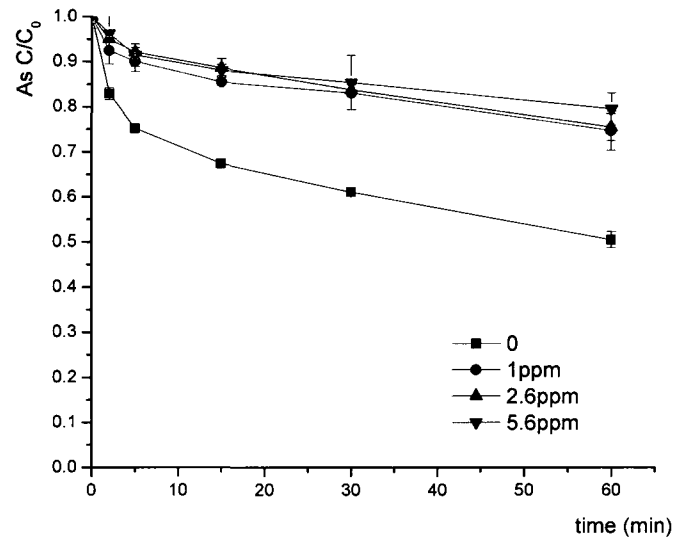
Figure 23 Arsenate removal efficiency on 0.1g/L nano magnetite vs. time with various conc. of citrate at pH=8 and

T=25°C.

4.2 Effect of Citrate on Ferric Hydroxide Nucleation

4.2.1 Inhibition of ferric hydroxide nucleation

Without any citrate, ferric hydroxide nucleation took place immediately after ferric nitrate was added. 2-line ferrihydrite was precipitated from the solution. The scanning electron microscope (SEM) image of the 2-line ferrihydrite prepared in this study shows poorly developed hexagonal crystalline particles whose lattice fringes are not easily recognized and many of the developed crystals aggregated together (Figure 24).
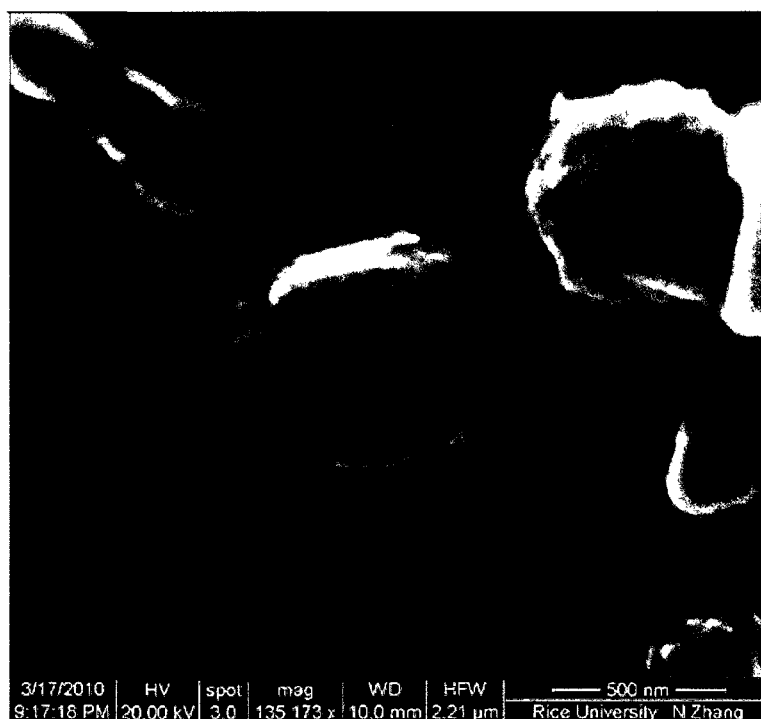
Figure 24 SEM image of 2-line ferrihydroxide in this study.

However, at an initial citrate to iron MR of 0.05 (i.e. corresponding to a citrate concentration of 1ppm), the iron concentration in the solution dropped by a few percent within the first minute, and then remained constant at about 95% of initial iron for the duration of the experiment (Figure 25). This inhibition of ferric hydroxide nucleation was found over the whole range of MR from 0.05 to 0.28, although a slight increase of iron concentration was observed as the initial citrate concentration increased. The iron nucleation inhibition pattern is similar to that with arsenate (Figure 21).

The period of the initial 5-7% drop of iron concentration is similar to the time that it takes for the pH to become stable after ferric nitrate addition (Figure 26). Ferric hydrolysis happens rapidly in water, resulting in a lower pH and a decrease of Fe (III) concentration. Therefore, a small part of the iron was lost from solution at the beginning of the reaction. Dynamic Liquid Scattering (DLS) was done to determine particle size in the sample containing iron and citrate after 1 hour and 3 days. The results were the same (Figure 27). The scattering intensities were lower than 1 kilocounts per second (kcps) for all samples with molar ratios of iron to citrate from 0.05 to 0.28. The intensities were too low to give a reliable particle size distribution.
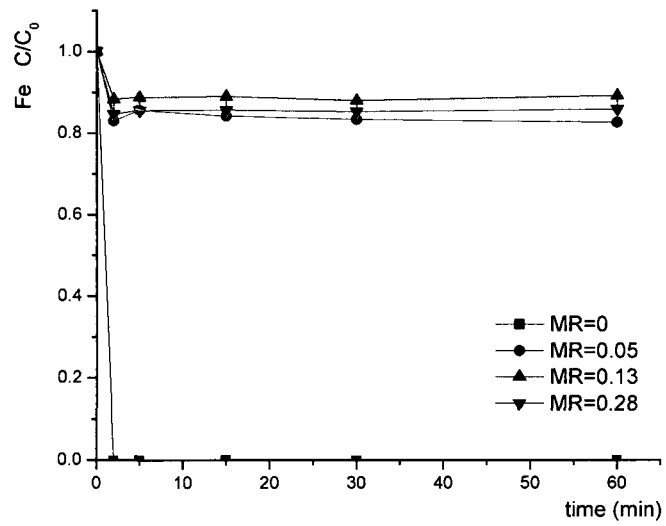
Figure 25   Ferric hydroxide nucleation vs. time in the presence of citrate with various MR at pH=8, T=25°C.
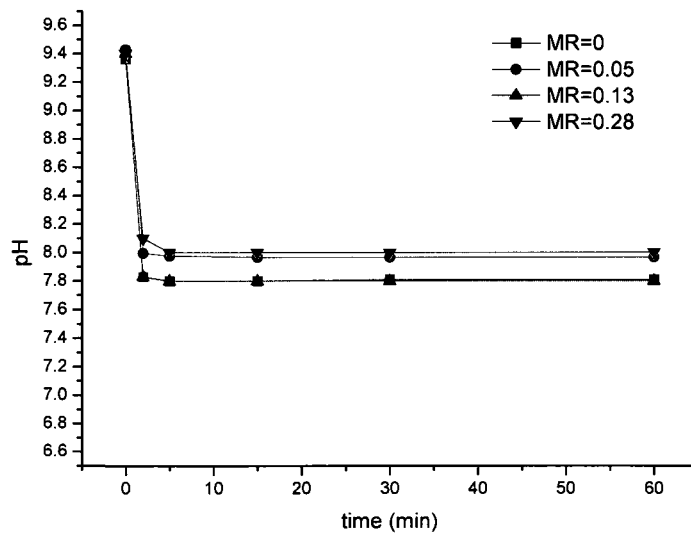
Figure 26 pH change vs. time after ferric nitrate addition.
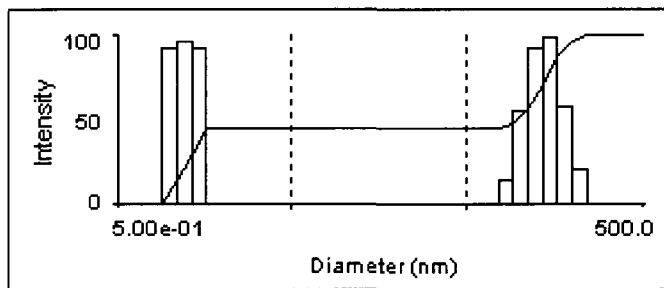
Figure 27 Signal intensity of DLS analysis for the solution after 3 days reaction with citric acid at pH=8, T=25°C.

The molar ratios of citrate to iron range from 0.02 to 10 in normal environmental conditions in water treatment plants. Low molar ratios (MR from 0.05 to 0.28; pH 8), were applied in this study, and citrate was found to effectively inhibit ferric hydroxide nucleation and precipitation. Models of inhibition of iron hydroxide nucleation that are based upon mononuclear and dinuclear iron citrate complex formation that have been used to describe the Fe (III) -citrate system at higher molar ratios (MR>1) cannot explain the inhibition of ferric nucleation by citrate at low molar ratios (MR<1), used in this study. However, it is possible that the inhibition of precipitation at low molar ratios of citrate to iron is caused by the formation of polynuclear complexes $Fe_{4-20}Cit$. The breakdown rate constants of ferric hydroxides become increasingly smaller as the molecular weight, or nuclearity, increases. Ferric hydroxide complex, $Fe_2(OH)_4^{4}+$ has a formation constant k_{12} of 630 $M^{-1}S^{-1}$, while its breakdown constant k_{21} (0.4 S^{-1}) is three orders of magnitude lower than k_{12} (Eq 4) (Cornell and Schwertmann 2003).

$$2Fe^{3+} + 2H_2O \underset{k_2}{\overset{k_{12}}{\rightleftarrows}} Fe_2(OH)_4^{4+} + H^+ \qquad \text{Equation 4}$$
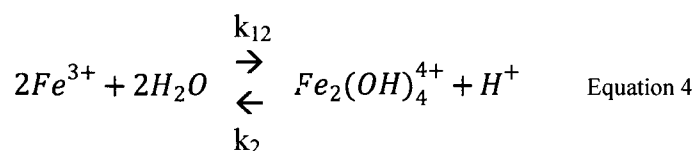
If there are not enough anions to stabilize the dimer structure ($Fe_2(OH)_4^{4}+$), further polymerization may happen rapidly (Bottero et al. 1994; Schwertmann et al. 1999). A macromolecular compound with composition $Na_5[Fe_{20}O_{20}(OH)_{13}Cit_3]$ has been isolated by membrane filtration (Spiro et al. 1967). Excess citrate prevented the formation of this macromolecular compound by forming an anionic chelate with two citrates. For 10^{-3} M iron solutions the presence of 0.02M citrate is enough to prevent detectable macromolecular compound (Spiro et al. 1967).

4.2.2 Effect of pH

Since the deprotonation may have a significant influence on ferric hydroxide nucleation, the citrate effect on retard ferric hydroxide nucleation was evaluated from pH 6 to 8 (Figure 28). Retardation of ferric hydroxide nucleation with the presence of citrate was performed as a function of pH. At lower MR, the iron concentration increased with an increasing pH from 6.0 to 8.0. The maximum ferric hydroxide inhibition nucleation (90%) occurred at pH 8.0 for the whole range of MRs. However, at pH 6 90% ferric hydroxide inhibition wasn't reached at any MR and at pH 7 90% inhibition was reached at MR= 0.10. In this study, the effect of pH on the nucleation retardation was more significant at higher pH values.
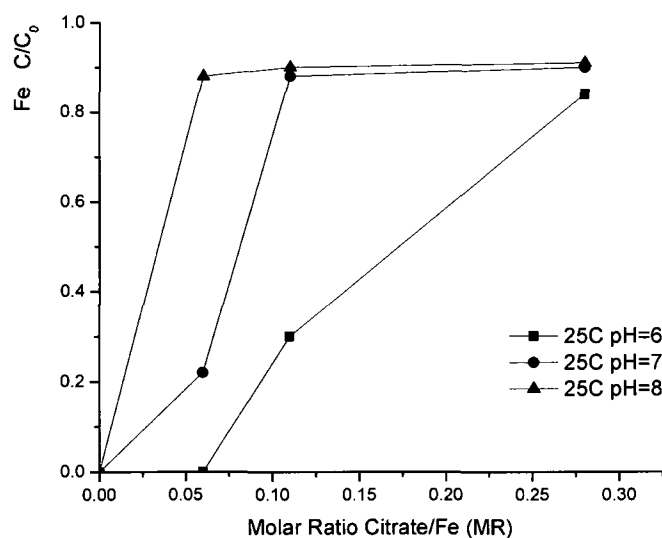
Figure 28 Ferric hydroxides nucleation vs. Molar Ratio of Citrate/Fe at pH 6 to 8.

4.2.3   Effect of functional groups on carboxylic acids

Six carboxylic acids which are stepwise products in the citric acid cycle (Krebs cycle) were selected to investigate the influence of functional groups on ferric hydroxide nucleation (Figure 29). Ferric hydroxide nucleation inhibition was greatest with citric acid, with three carboxyl groups (-COOH) and one hydroxyl group (-OH), while negligable effect was observed in the presence of the other six carboxylic acids over the molar ratio range of 0 to 0.28. Citric acid inhibited 91% ferric hydroxide nucleation at a MR of 0.13 and the inhibition effect slightly increased with citric acid addition (Yean 2007)(Table 6).
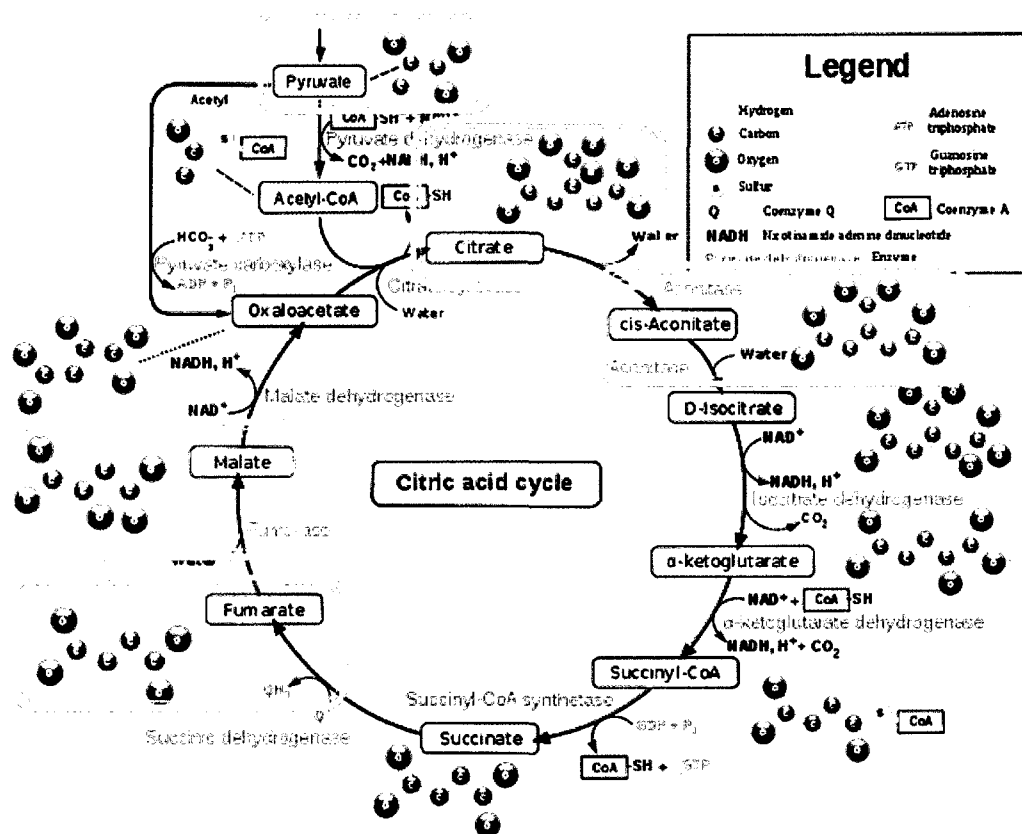
Figure 29 A schematic of citric acid cycle and the carboxylic acids used in this study was labeled with orange frame (Narayanese and WikiUserPedia 2008).

A change in structure always leads a change in function. For cis-aconitic acid trans-aconitic acid and fumaric acid, the C=C group may not give enough space to rotate and complex with iron. For pyruvic acid the ketone group (=O) may limit the combination with iron. However, malic acid with only -COOH and -OH groups didn't show any inhibitor effect.

On the other hand, DL-tartaric acid with the same kinds of function groups as citric acid prevented 7% precipitation of ferric hydroxides at an initial MR of 0.13, and 91% at an initial MR of 0.28. The inhibition effect became more significant when more DL-tartaric acid was added in the system.

Carboxylic acid	Fe Conc. in solution(%)		
	MR=0	0.13	0.28
cis-Aconitic acid	0	0	0
trans-Aconitic acid	0	0	0
Fumaric acid	0	0	0
Malic acid	0	0	0
Pyruvic acid	0	0	0
Citric acid	0	91%	94%
DL-tartaric acid	0	7%	91%

Table 6   Fe concentration in the solution after 1 hour reaction with different carboxylic acids at pH=8, T=25°C.

4.3   Non-crystalline macromolecular complex

4.3.1   Mass spectra analysis of Fe-citrate complex

ESI-TOFMS spectra for the molecular ions having the Fe isotopic signature and elctrospray ionization conditions were optimized by method Rellan-Alvarez published (Rellan-Alvarez et al. 2008). Full scan mass spectra were recorded (m/z 100-1500, scan time) in both positive and negative ion polarity modes with a molar ratio of citrate to iron 0.28. An average mass spectrum in positive ion mode shows major features at m/z 353.3, 381.3, 659.3, 711.6, 739 from m/z= 300 to 1200. The signal only at m/z 659.3 shows a characteristic isotope pattern of a single charged 4:1 complex Fe_4Cit^+ ($[Fe_4O_{22}C_6H_{12}]^+$) (Figure 30 and Figure 31 b). The calculated isotopic distribution is comparably shown in Figure 31 a. A main peak is at 659.3, and three minor peaks at two sides of the main peak are due to the presence of ^{54}Fe isotope, which is a characteristic of an iron complex. This Fe-citrate complex with molecular weight of 659.3 can be assigned as $[Fe_4O_{13}H_3Cit \cdot 2H_2O]^+$. No Fe characteristic isotopic was detected at other major peaks.

Citrate signal was recorded at an average mass spectrum at m/z 381.0. The present of citrate peak implies excess citrate in the solution which wasn't combined with iron (Figure 30 and Figure 32 b). This peak can be assigned to a citrate dimer, $Cit_2H_3^+$, although the structure needs to be confirmed. The calculated isotopic distribution is comparably shown in Figure 32 a. The intensity of citrate is around twice higher than the intensity of Fe_4Cit complex, but it is not enough for quantitative analysis since ESI-MS is more widely used in qualitative than quantitative analysis. Therefore, the result suggests there is free citrate left in the solution.

Potentiometric and spectrophotometric titrations suggested that FeCit and Fe_2Cit_2 complexes exist in aqueous solution at high molar ratio of citrate to iron (MR=2.6-10) and at a large pH range (pH=1.5-7) (Konigsberger et al. 2000; Hamada et al. 2006). ESI-MS not only confirmed the existence of monomer ($FeCit_{1-4}$) and dimer complex (Fe_2Cit_2), but suggested trimer (Fe_3Cit_{3-4}) also can be identified to coexist in the aqueous phase (Isabelle et al. 2005; Rellan-Alvarez et al. 2008; Volker and Bernhard 2009). However, there is not such a large molar excess of citrate in the water treatment plant. In summary, at a low molar ratio of citrate to iron, Fe atoms associate with nearly all of the citrate molecules and become complexes and the footprint of Fe_4Cit complex has been caught by ESI-TOFMS.
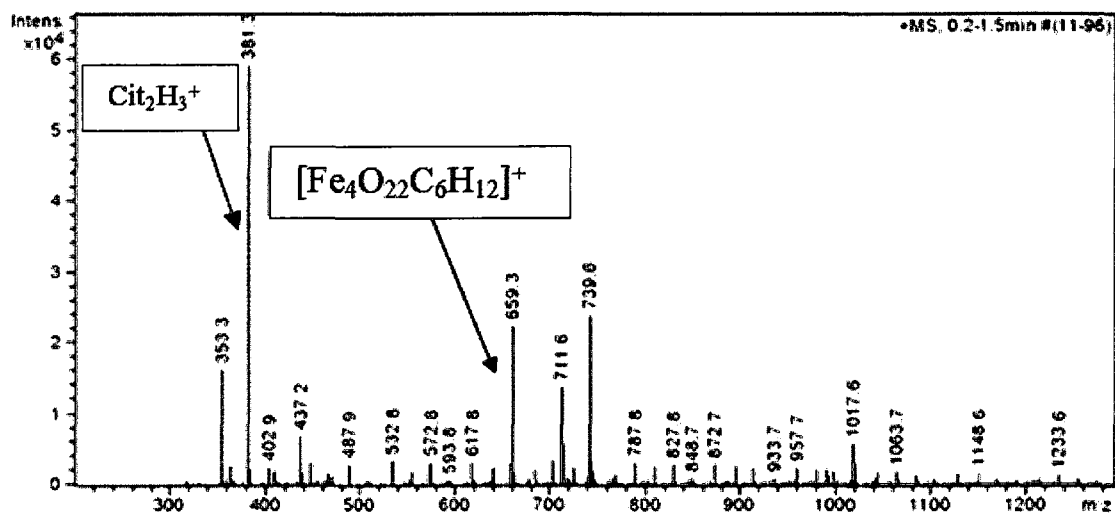
Figure 30 ESI mass spectra of aqueous solution at a citrate/Fe molar ration of 0.25 in the positive ion mode.
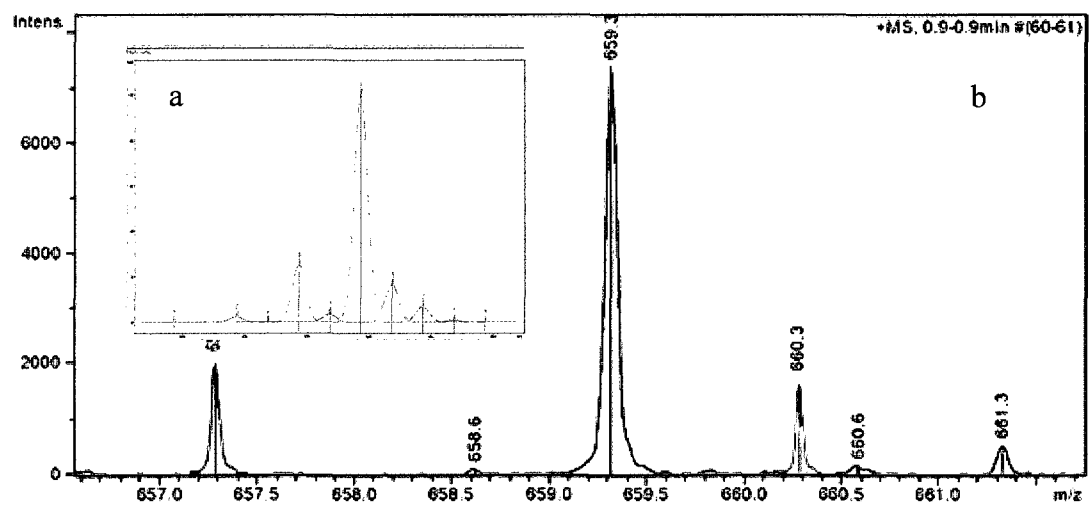
Figure 31 Theoretical (a) and Experimental (b) ESI mass spectra of $[Fe_4O_{13}H_3Cit \cdot 2H_2O]^+$
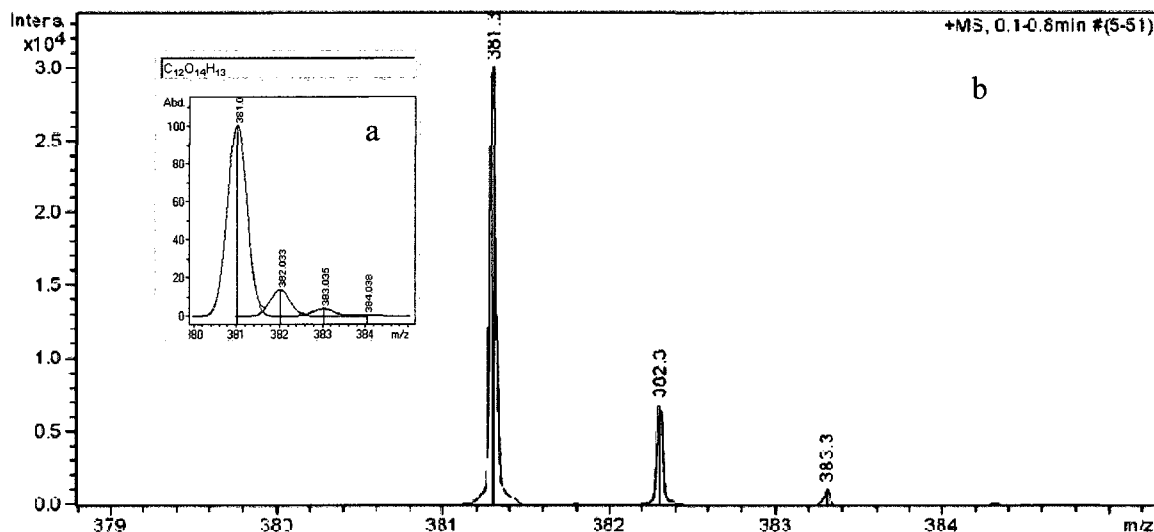
Figure 32 Theoretical (a) and Experimental (b) ESI mass spectra of $Cit_2H_3^+$.

4.3.2 Fe₄Cit complex, molecular modeling

A Fe₄Cit complex was modeled as a tetra-nuclear Fe oxobridged complex by Density Functional Theory (DFT), a standard method for quantum chemical modeling of transition metals and the convergence of the wavefunction was achieved after optimization. According to the result of ESI-MS, the complex formula can be written as $FeO(Fe_3O_{12}H_{12})Cit$. One central tetrahedrally coordinated Fe is connected to three edge-sharing octahedrally coordinated Fe atoms by μ_4-oxo bridges and is also bonded to a citrate molecule by three carboxylate groups (Figure 33). All Fe atoms have a slightly distorted configuration.

An initial guess of Fe₄Cit complex molecular model was obtained by the knowledge of the iron carboxylates formation in aqueous Fe systems. This optimized Fe₄Cit structure contains both octahedral and tetrahedral sites, which is closely related to

one part of the Baker-Figgis-Keggin cluster. However, only one trimeric groups of $Fe(O)_6$ octahedra is connected to the tetrahedral Fe atom in Fe_4Cit structure rather than four octahedral groups bonded to the central tetrahedral Fe atom in a complete Baker-Figgis Keggin structure. The other three positions of the tetrahedral Fe atom are occupied by citrate complexation. A complete Keggin Fe_{13} structure was proposed by Michel et al. in 2007 for nanocrystalline ferrihydrite without any citrate and with a citrate to iron molar ratio of 0.03(Michel et al. 2007; Michel et al. 2009).

The possible interference pathway of citrate in ferric hydroxides nucleation inhibition at low molar ratios of citrate to iron can be depicted as follows. 1) At a molar ratio of citrate to iron <0.05, citrate can affect the dominate species of ferric hydroxides formed in solutions, but citrate has little effect on ferric hydroxides nucleation inhibition (Krishnamurti and Huang 1991). 2) At a molar ratio of citrate to iron from 0.05 to 1, the citrate molecule can prevent further condensation by association of organic ligand with ferric hydroxide. Ferric hydroxide cluster is stabilized in solutions by citrate as a macromolecular compound. Generally, the strong affinities to Fe (III) of the citrate anions apparently change or prevent the Fe-O-Fe or Fe-OH-Fe bond formation resulting in precipitation.
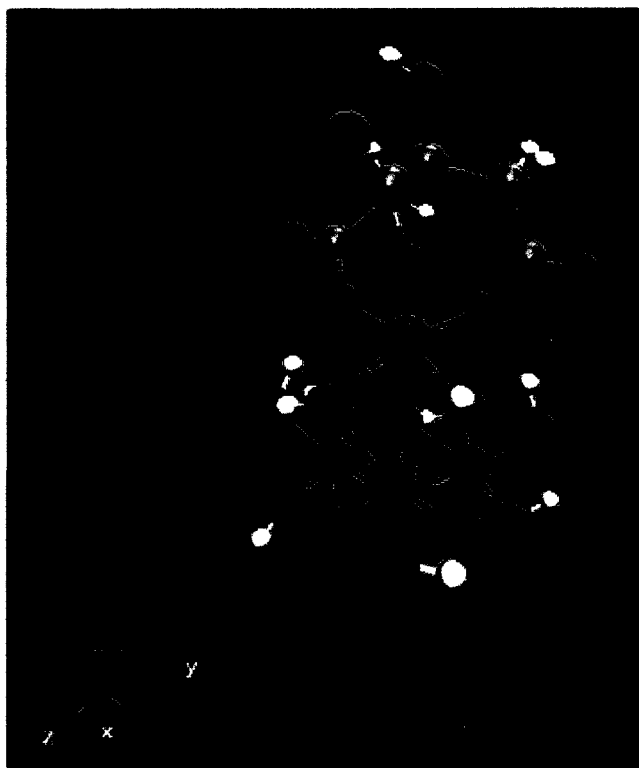
Figure 33 Proposed structure for Fe₄Cit found in solution sample. Iron, oxygen, carbon and hydrogen atoms are shown in green, red, cyan, and white, respectively.

5 Conclusion and future work

5.1 Conclusion

Arsenic in drinking water is becoming a worldwide health concern. Ferric salts precipitation/coagulation method is applied in most water treatment plants (U.S.EPA 2002). A novel nanomagnetite adsorption method is recommended as a promising method for home water treatment system (Yavuz et al. 2006; Shipley et al. 2009).

This work discussed the citrate effect on arsenate removal at low molar ratios of citrate to iron (MR<1). Citrate was demonstrated to most effectively inhibit arsenate removal among 7 carboxylic acids. 90% and 50% arsenate removal inhibition was found for the ferric salts precipitation method and the nanomagnetite adsorption method, respectively (Figure 34), and the maximum inhibition was reached at MR=0.05. The inhibition effect is more significant at pH 6 than pH 8.

For ferric salts precipitation method, a stable Fe_4Cit complex ($FeO(Fe_3O_{12}H_3)Cit$) was identified by ESI-MS, which prevented the further growth of keggin-like ferric hydroxide unit and the nucleation of ferric hydroxide. Therefore, both the ferric hydroxide and attached arsenate cannot precipitate from the solutions. The optimized structure of Fe_4Cit complex is closely related to one part of the Baker-Figgis-Keggin cluster. For nanomagnetite adsorption method in this study, the adsorption of arsenate and citrate onto nanomagnetite involved not the competition for binding sites, but the cooperation between the two species. The cooperation effect causes a lower adsorption affinity of arsenate to the water-magnetite interface, therefore the inhibition of arsenate removal.

According the significant inhibition of arsenate removal shown in this work, the levels of citrate is suggested to be monitored in water treatment plants, in order to get an ideal arsenate removal.

• Ferric Salts Percipitation/ Coagulation Method

As & Cit

$FeO(Fe_3O_{12}H_3)Cit$

•The keggin-like iron hydroxide unit is terminated furture growth by adsorbed citrate, so the ferric hydroxide is stabilized in solutions.

• Arsenate is adsorbed to stabilized colloides, such as $FeO(Fe_3O_{12}H_3)Cit$, but not can not be seperated and removed from water.

90% As removal inhibition

a)

• Nanomagnetite Adsorption Method

As & Cit

As-Cit
Fe-Cit-As

•The adsorption of As and Cit onto nanomagnetite involved not only competition for binding sites, but also the cooperation between the two species.

•The cooperation between As and Cit causes a lower adsorption affinity to the water-magnetite interface.

50% As removal inhibition

b)

Figure 34 Mechanism of negative effect of citrate on arsenic removal efficiency with a) Ferric salt precipitation/coagulation method and b) Nanomagnetite adsorption method.

6 References

Ahmed, M. F. (2001). An Overview of Arsenic Removal Technologies in Bangladesh and India, Bangladesh University of Engineering and Technology and the United Nation University.

Ahmed, M. F., et al., Eds. (2001). Technologies for Arsenic Removal from Drinking Water, Bangladesh University of Engineering and Technology and the United Nation University.

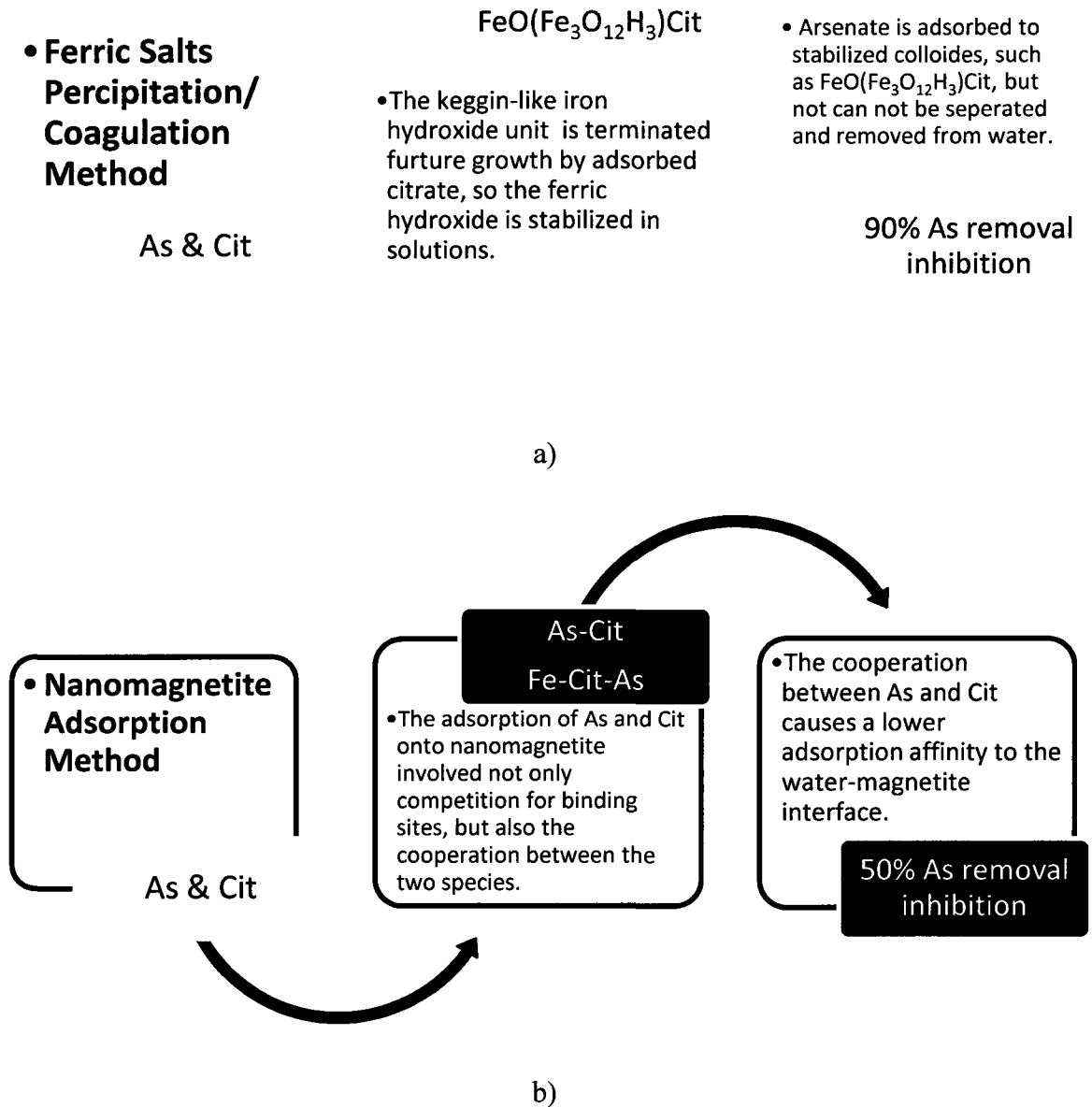Anderson, P. R. and M. M. Benjamin (1985). "Effect of silicon on the crystallization and adsorption properties of ferric oxides." Environmental Science & Technology 19(11): 1048-1053.

Benali, O., et al. (2001). "Effect of orthophosphate on the oxidation products of Fe(II)-Fe(III) hydroxycarbonate: the transformation of green rust to ferrihydrite." Geochimica et Cosmochimica Acta 65(11): 1715-1726.

Bentley, R. and T. G. Chasteen (2002). "Microbial Methylation of Metalloids: Arsenic, Antimony, and Bismuth." Microbiology and Molecular Biology Reviews 66(2): 250-271.

Betts, K. S. (2001). "Technology Solutions: Developing a good solution for arsenic." Environmental Science & Technology 35(19): 414A-415A.

Beuhler, R. J., et al. (1974). "Proton Transfer Mass Spectrometry of Peptides.A Rapid Heating Technique for Underivatized Peptides Containing Arginine." Journal of American Chemistry Society 96(12): 3990.

Bigham, J. M., et al. (1994). "Schwertmannite, a new iron oxyhydroxysulfate from Pyhasalmi, Finland, and other localities." Mineral Magazine 58: 641-664.

Bigham, J. M., et al. (1996). "Schwertmannite and the chemical modeling of iron in acid sulfate waters." Geochimica et Cosmochimica Acta 60(12): 2111-2121.

Bino, A., et al. (2002). "Synthesis and Structure of [Fe13O4F24(OMe)12]5-: The First Open-Shell Keggin Ion." Journal of the American Chemical Society 124(17): 4578-4579.

Bottero, J. Y., et al. (1987). "Mechanism of formation of aluminum trihydroxide from keggin Al13 polymers." Journal of Colloid and Interface Science 117(1): 47-57.

Bottero, J. Y., et al. (1994). "Structure and mechanisms of formation of iron oxide hydroxide (chloride) polymers." Langmuir 10(1): 316-319.

Buerge, I. J. and S. J. Hug (1998). "Influence of Organic Ligands on Chromium(VI) Reduction by Iron(II)." Environmental Science & Technology 32(14): 2092-2099.

Casey, W. H. (2005). "Large Aqueous Aluminum Hydroxide Molecules." Chemical Reviews 106(1): 1-16.

Caudle, M. T., et al. (1994). "Electrospray Mass Spectrometry Study of 1:1 Ferric Dihydroxamates." Inorganic Chemistry 33(5): 843-844.

Chen, Y. and H. Ahsan (2004). "Cancer Burden From Arsenic in Drinking Water in Bangladesh." American Journal of Public Health 94(5).

Chiou, H. Y., et al. (1995). "Incidence of internal cancers and ingested inorganic arsenic: a seven-year follow-up study in Taiwan." Cancer Research 15(55): 1296-1300.

Chuckrov, F. V. and B. B. Zvyagin (1973).

Consta, S., et al. (2003). "Fragmentation mechanisms of aqueous clusters charged with ions." The Journal of Chemical Physics 119(19): 10125-10132.

Cornell, R. M. and U. Schwertmann (1979). "Influence of organic anions on the crystallization of ferrihydrite." Clays and Clay Minerals 27(6): 402-410.

Cornell, R. M. and U. Schwertmann (2003). The Iron Oxides: Structure, Properties, Reactions, Occurrences and Uses. Weinheim, WILEY-VCH.

Cragg, P. (2005). A Practical Guide to Supramolecular Chemistry. West Sussex, John Wiley & Son Ltd.

Cram, D. J. and J. M. Cram (1994). Container Molecules and their Guests. Great Britain, The Royal Society of Chemistry.

Crecelius, E. A. (1977). "Changes in the chemical speciation of arsenic following ingestion by man." Environmental Health Perspectives 19: 147-150.

Del Razo, L. M., et al. (2002). "Arsenic levels in cooked food and assessment of adult dietary intake of arsenic in the Region Lagunera, Mexico." Food and Chemical Toxicology 40(10): 1423-1431.

Dixit, S. and J. G. Hering (2003). "Comparison of Arsenic(V) and Arsenic(III) Sorption onto Iron Oxide Minerals: Implications for Arsenic Mobility." Environmental Science & Technology 37(18): 4182-4189.

Dole, M., et al. (1968). "Molecular Beams of Macroions." The Journal of Chemical Physics 49(5): 2240-2249.

Drits, V. A., et al. (1993). "Structure of feroxyhite as determined by simulation of X-ray diffraction curves." Clay Minerals 28(2): 209-222.

Edwards, M. (1994). "Chemistry of Arsenic Removal During Coagulation and Fe-Mn Oxidation." Journal-American Water Works Association 86(9): 64-78.

El Samrani, A. G., et al. (2006). "Behavior of complexing ligands during coagulation and flocculation by ferric chloride: A comparative study between sewage water and an engineered colloidal model." Journal of Environmental Engineering & Science 5(5): 397-404.

Evans, R., et al. (2008). "Nature of non-transferrin-bound iron: studies on iron citrate complexes and thalassemic sera." Journal of Biological Inorganic Chemistry 13(1): 57-74.

Farrell, J. W. (2009). Nanomagnetite Enhances Sand Filtration for Removal of Arsenic From Drinking Water. Civil and Environmetnal Department. Houston, Rice University. M.S.

Feenstra, L., et al. (2007). Arsenic in groundwater: Overview and evaluation of removal methods. Utrecht, International groundwater resources assessment centre.

Fenn, J. B. (2000). Improved method and apparatus for electrospray ionization. E. P. Office. EP1010468 (A1)

Fenn, J. B., et al. (1989). "Electrospray ionization for mass spectrometry of large biomolecules." Science 246(4926): 64-71.

Ferguson, A. D., et al. (2002). "Structural Basis of Gating by the Outer Membrane Transporter FecA." Science 295(5560): 1715-1719.

Feynman, R. P. (1960). "There's Plenty of Room at the Bottom." Engineering and Science 23(22).

Fields, K. A., et al. (2000). Arsenic Removal from Drinking Water by Coagulation/Filtration and Lime Softening Plants. Columbus, U.S., Battelle.

Flynn, C. M. (1984). "Hydrolysis of inorganic iron(III) salts." Chemical Reviews 84(1): 31-41.

Focazio, M. J., et al. (2000). A Retrospective Analysis on the Occurrence of Arsenic in Ground-Water Resources of the United States and Limitations in Drinking-Water-Supply Characterizations. Reston, U.S.Geological Survey.

Frankenberger, W. T., Jr., Ed. (2001). Environmental chemistry of arsenic. New York Basel, Marcel Dekker, Inc.

Furrer, G., et al. (2002). "The Origin of Aluminum Flocs in Polluted Streams." Science 297(5590): 2245.

Furukawa, Y., et al. (2002). "Formation of Ferrihydrite and Associated Iron Corrosion Products in Permeable Reactive Barriers of Zero-Valent Iron." Environmental Science & Technology 36(24): 5469-5475.

Garelick, H., et al. (2005). "Remediation Technologies for Arsenic Contaminated Drinking Waters." Journal of Soils and Sediments 5(3): 182-190.

Garelick, H. and H. Jones (2008). "Mitigating Arsenic Pollution: Bridging the Gap Between Knowledge and Practice." Chemistry International 30(4).

Gomez-Caminero, A., et al. (2001). Arsenic and Arsenic Compounds. Geneva, World Health Organization.

Gouzerh, P. and M. Che (2006). "From Scheele and Berzelius to Müller: polyoxometalates (POMs) revisited and the "missing link" between the bottom up and top down approaches." L'Actualité Chimique 298(9): 1-14.

Grafe, M., et al. (2002). "Adsorption of Arsenate and Arsenite on Ferrihydrite in the Presence and Absence of Dissolved Organic Carbon." J Environ Qual 31(4): 1115-1123.

Greenwood, N. N. and A. Earnshaw (1997). Chemistry of the elements. Boston, Oxford.

Hamada, Y. Z., et al. (2006). "Accurate Potentiometric Studies of Chromium-Citrate and Ferric-Citrate Complexes in Aqueous Solutions at Physiological and Alkaline pH Values." Synthesis and Reactivity in Inorganic, Metal-Organic, and Nano-Metal Chemistry 36(6): 469 - 476.

Hamada, Y. Z., et al. (2003). "Potentiometric and UV-Vis Spectroscopy Studies of Citrate with the Hexaquo Fe^{3+} and Cr^{3+} Metal Ions." Synthesis and Reactivity in Inorganic, Metal-Organic, and Nano-Metal Chemistry 33(8): 1425 - 1440.

Harvey, C. F., et al. (2002). "Arsenic Mobility and Groundwater Extraction in Bangladesh." Science 298(5598): 1602-1606.

Helsel, D. (2000). Arsenic in Ground-Water Resources of the United States, U.S. Geological Survey.

Hendrik, N., et al. (2002). "Speciation of Fe(III)-chelate complexes by electrospray ionization ion trap and laser desorption/ionization Fourier transform ion cyclotron resonance mass spectrometry." Rapid Communications in Mass Spectrometry 16(16): 1556-1561.

Hering, J. G., et al. (1997). "Arsenic Removal from Drinking Water during Coagulation." Journal of Environmental Engineering 123(8): 800-807.

Howard, G. (2003). Arsenic, Drinking-water and Health Risk Substitution in Arsenic Mitigation: a Discussion Paper. Geneva, WHO.

Iribarne, J. V. and B. A. Thomson (1976). "On the evaporation of small ions from charged droplets." Journal of Chemistry Physics 64: 2287.

Isabelle, G.-L., et al. (2005). "New Trends in the Chemistry of Iron(III) Citrate Complexes: Correlations between X-ray Structures and Solution Species Probed

by Electrospray Mass Spectrometry and Kinetics of Iron Uptake from Citrate by Iron Chelators." Chemistry - A European Journal **11**(7): 2207-2219.

Janney, D. E., et al. (2000). "Structure of synthetic 2-line ferrihydrite by electron nanodiffraction." American Mineralogist **85**(9): 1180-1187.

Janney, D. E., et al. (2000). "TRANSMISSION ELECTRON MICROSCOPY OF SYNTHETIC 2- AND 6-LINE FERRIHYDRITE." Clays and Clay Minerals **48**(1): 111-119.

John, B. F. (2003). "Electrospray Wings for Molecular Elephants (Nobel Lecture)13." Angewandte Chemie International Edition **42**(33): 3871-3894.

Keggin, J. F. (1933). "Structure of the molecule of 12-phosphotungstic acid." Nature **131**(3321): 908-909.

Konigsberger, L. C., et al. (2000). "Complexation of iron(III) and iron(II) by citrate. Implications for iron speciation in blood plasma." Journal of Inorganic Biochemistry **78**: 175-184.

Krishnamurti, G. S. R. and P. M. Huang (1991). "Influence of citrate on the kinetics of Fe(II) oxidation and the formation of iron oxyhydroxides." Clays and Clay Minerals **39**(1): 28-34.

Lievremont, D., et al. (2009). "Arsenic in contaminated waters: Biogeochemical cycle, microbial metabolism and biotreatment processes." Biochimie **91**(10): 1229-1237.

Liu, C. and P. M. Huang (2003). "Kinetics of lead adsorption by iron oxides formed under the influence of citrate." Geochimica et Cosmochimica Acta **67**(5): 1045-1054.

Long, D. L., et al. (2007). "Polyoxometalate clusters, nanostructures and materials: From self assembly to designer materials and devices." Chemical Society Reviews **36**(1): 105-121.

Lytle, D. A., et al. (2004). "Accumulation of Arsenic in Drinking Water Distribution Systems." Environmental Science & Technology **38**(20): 5365-5372.

M. Grafe, M. J. E., P. R. Grossl (2001). "Adsorption of arsenate (V) and arsenite (III) on goethite in the presence and absence of dissolved organic carbon." Soil Sci. Soc. Am. J. **65**(6): 1680-1687

Manceau, A. (2009). "Evaluation of the structural model for ferrihydrite derived from real-space modelling of high-energy X-ray diffraction data." Clay Minerals **44**(1): 19-34.

Mandal, B. K. and K. T. Suzuki (2002). "Arsenic round the world: a review." Talanta **58**(1): 201-235.

Martin, B. R. (1986). "Citrate binding of Al^{3+} and Fe^{3+}." Journal of Inorganic Biochemistry **28**: 181-187.

McArthur, J. M., et al. (2001). "Arsenic in Groundwater: Testing Pollution Mechanisms for Sedimentary Aquifers in Bangladesh." Water Resour. Res. **37**(1): 109-117.

McGregor, S. J. and B. J. H. (1992). "Effect of pH and Citrate on Binding of Iron and Gallium by Transferrin in Serum." Clinical Chemistry.

McNeill, L. S. and M. Edwards (1995). "Soluble arsenic removal at water treatment plants." Journal-American Water Works Association **87**(4): 105-113.

McNeill, L. S. and M. Edwards (1996). "Predicting As removal during metal hydroxide precipitation." Journal-American Water Works Association.

Michel, F. M., et al. (2009). "Ordered ferrimagnetic form of ferrihydrite reveals links among structure, composition, and magnetism." Proceedings of the National Academy of Sciences 107(7): 2787-2792.

Michel, F. M., et al. (2010). "Ordered ferrimagnetic form of ferrihydrite reveals links among structure, composition, and magnetism." Proceedings of the National Academy of Sciences 107(7): 2787-2792.

Michel, F. M., et al. (2007). "The Structure of Ferrihydrite, a Nanocrystalline Material." Science 316(5832): 1726-1729.

Michel, F. M., et al. (2007). "Similarities in 2- and 6-Line Ferrihydrite Based on Pair Distribution Function Analysis of X-ray Total Scattering." Chemistry of Materials 19(6): 1489-1496.

Mladenov, N., et al. (2009). "Dissolved Organic Matter Sources and Consequences for Iron and Arsenic Mobilization in Bangladesh Aquifers." Environmental Science & Technology 44(1): 123-128.

Muller, A. (2003). "CHEMISTRY: The Beauty of Symmetry." Science 300(5620): 749-750.

Narayanese and WikiUserPedia. (2008). "Citric acid cycle." from http://en.wikipedia.org/wiki/File:Citric_acid_cycle_noi.svg.

Nguyen, S. and J. B. Fenn (2007). "Gas-phase ions of solute species from charged droplets of solutions." Proceedings of the National Academy of Sciences 104(4): 1111-1117.

Paul, K. and H. V. Udo (2009). "Electrospray: From ions in solution to ions in the gas phase, what we know now." Mass Spectrometry Reviews 28(6): 898-917.

Pelley, J. (2009). "Arsenic in rice: a recipe for nutrient loss." Environmental Science & Technology 43(21): 8004-8004.

Penn, R. L. (2007). "CHEMISTRY: Resolving an Elusive Structure." Science 316(5832): 1704-1705.

Pope, M. T. and A. Muller (1991). "Polyoxometalate Chemistry: An Old Field with New Dimensions in Several Disciplines." Angewandte Chemie International Edition in English 30(1): 34-48.

Rasmussen, L. and K. J. Andersen (2000). Chapter 2: Environmetal Health and human exposure assessment. United Nations Synthesis Report on Arsenic in Drinking Water, Unites Nations.

Rellan-Alvarez, R., et al. (2008). "Identification of a Tri-Iron(III), Tri-Citrate Complex in the Xylem Sap of Iron-Deficient Tomato Resupplied with Iron: New Insights into Plant Iron Long-Distance Transport." Plant Cell Physiol. 51(1): 91-102.

Rose, A. L. and T. D. Waite (2003). "Kinetics of iron complexation by dissolved natural organic matter in coastal waters." Marine Chemistry 84(1-2): 85-103.

Rose, J., et al. (1997). "Structure and Mechanisms of Formation of FeOOH(NO3) Oligomers in the Early Stages of Hydrolysis." Langmuir 13(12): 3240-3246.

Saha, J. C., et al. (1999). "A Review of Arsenic Poisoning and its Effects on Human Health." Critical Reviews in Environmental Science and Technology 29(3): 281 - 313.

Schalley, C. A., Ed. (2007). Analytical Methods in Supramolecular Chemistry. KGaA, Weinheim, WILEY-VCH.

Schwertmann, U. and R. M. Cornell (2000). Iron Oxides in the Laboratory: preparation and Characterization. Weinheim, WILEY-VCH.

Schwertmann, U., et al. (1999). "From Fe(III) Ions to Ferrihydrite and then to Hematite." Journal of Colloid and Interface Science 209(1): 215-223.

Shanbrom, E. (2005). Enhanced iodine treatment of drinking water. U. S. Patent. the U.S.A., Hartley, Michael G. 6863905.

Shipley, H. J., et al. (2009). "ADSORPTION OF ARSENIC TO MAGNETITE NANOPARTICLES: EFFECT OF PARTICLE CONCENTRATION, pH, IONIC STRENGTH, AND TEMPERATURE." Environmental Toxicology and Chemistry 28(3): 509-515.

Shweky, I., et al. (1994). "Syntheses, Structures, and Magnetic Properties of Two Dinuclear Iron(III) Citrate Complexes." Inorganic Chemistry 33(23): 5161-5162.

Smedley, P. L. and D. G. Kinniburgh (2002). "A review of the source, behavior and distribution of arsenic in natural waters." Applied Geochemistry 17(52): 517-568.

Sombo, Y. (2000). Chapter 5: Drinking Water Guidelines and Standards. United Nations Synthesis Report on Arsenic in Drinking Water. Geneva, Unite Nations.

Sorg, T. J. and G. S. Logsdon (1978). "Treatment Technology to Meet the Interim Primary Drinking

Water Regulations for Inorganics: Part 2." Journal-American Water Works Association 7: 379-392.

Spiro, T. G., et al. (1967). "Hydrolytic polymerization of ferric citrate. II. Influence of excess citrate." Journal of the American Chemical Society 89(22): 5559-5562.

Spiro, T. G., et al. (1967). "Hydrolytic polymerization of ferric citrate. I. Chemistry of the polymer." Journal of the American Chemical Society 89(22): 5555-5559.

Spiro, T. G. and P. Saltman, Eds. (1969). Polynuclear complexes of iron and their biological implications. Structure and Bonding, Springer Berlin / Heidelberg.

Steed, J. W. and J. L. Atwood (2000). Supramolecular Chemistry. Chichester, John Wiley & Sons. Ltd.

Thomas, D. J., et al. (2007). "Arsenic (+3 Oxidation State) Methyltransferase and the Methylation of Arsenicals." Experimental Biology and Medicine 232(1): 3-13.

Thomas, D. J., et al. (2010). "Arsenic (+ 3 Oxidation State) Methyltransferase and the Methylation of Arsenicals in the Invertebrate Chordate Ciona intestinalis." Toxicol. Sci. 113(1): 70-76.

Tianbo, L., et al. (2004). "Self-Assembly in Aqueous Solution of Wheel-Shaped Mo_{<FONT SIZE='-1'>154</FONT>} Oxide Clusters into Vesicles." ChemInform 35(5).

Tomson, B. A. and J. V. Iribarne (1979). "Field induced ion evaporation from liquid surfaces at atmospheric pressure." Journal of Chemistry Physics 71: 4451.

U.S.EPA (2000). Technologies and Costs for Removal of Arsenic from Drinking Water.

U.S.EPA (2002). Arsenic Treatment Technologies for Soil, Wast, and Water. Cincinnati,U.S.

U.S.EPA (2008). Citric Acid, and Salts Summary Document: Registration Review.

Ui, J., Ed. (1992). Industrial Pollution in Japan. Tokyo, United Nations University Press.

UNicef (1998). The State of the World's Children. New York Geneva, Oxford University Press.

Unicef (2008). UNICEF Handbook on Water Quality. New York, United Nations Children's Fund.

Valerio, B. D. M. and G. G. Bombi (2006). "Electrospray mass spectrometry (ESI-MS) in the study of metal-ligand solution equilibria." Mass Spectrometry Reviews 25(3): 347-379.

Van der Woude, J. H. A., et al. (1984). "Formation of colloidal dispersions from supersaturated iron(III) nitrate solutions. IV. Analysis of slow flocculation of goethite." Colloids and Surfaces 11(3-4): 391-400.

Vance, D. B. (1995). "Arsenic chemical behavior and treatment." National Environmental Journal 5(3): 60-64.

Violante, A., et al. (2007). "Coprecipitation of Arsenate with Metal Oxides. 2. Nature, Mineralogy, and Reactivity of Iron(III) Precipitates." Environmental Science & Technology 41(24): 8275-8280.

Violante, A., et al. (2009). "Coprecipitation of Arsenate with Metal Oxides. 3. Nature, Mineralogy, and Reactivity of Iron(III)-Aluminum Precipitates." Environmental Science & Technology 43(5): 1515-1521.

Volker, N. and M. Bernhard (2009). "Electrospray ionisation with selected reaction monitoring for the determination of Mn-citrate, Fe-citrate, Cu-citrate and Zn-citrate." Rapid Communications in Mass Spectrometry 23(15): 2338-2346.

Whitehouse, C. M., et al. (1985). "Electrospray Interface for Liquid Chromatographs and Mass Spectrometers." Journal of American Chemistry Society 57(3): 675-679.

Wilson, R. (2009). "Chronic Arsenic Poisoning: History, Study and Remediation." from http://www.physics.harvard.edu/~wilson/arsenic/arsenic_project_introduction.html.

Xu, Y., et al. (2008). "Clinical Manifestations and Arsenic Methylation after a Rare Subacute Arsenic Poisoning Accident." Toxicol. Sci. 103(2): 278-284.

Yan, B., et al. (2005). "Nitrate Removal from Drinking Water with Sodium Citrate as Sole Carbon Source." TRANSACTIONS OF TIANJIN UNIVERSITY 11(1).

Yavuz, C. T., et al. (2006). "Low-Field Magnetic Separation of Monodisperse Fe3O4 Nanocrystals." Science 314(5801): 964-967.

Yean, S. (2007). Carboxylic Acids Effect on Ferric Hydroxide Nucleation. Houston, Rice Universtiy.

Yu, W. H., et al. (2003). "Arsenic in groundwater in Bangladesh: A geostatistical and epidemiological framework for evaluating health effects and potential remedies." Water Resour. Res. 39.